Leeghwaterstraat 44
2628 CA Delft
P.O. Box 6012
2600 JA Delft
The Netherlands

www.tno.nl

T +31 88 866 22 00
F +31 88 866 06 30

TNO report

TNO 2017 R10528 | 1.1

Literature search on screening for flow-induced vibrations on hydraulic gates

Date	17 October 2017
Author(s)	S. Belfroid
Copy no	
No. of copies	
Number of pages	77 (incl. appendices)
Number of appendices	
Sponsor	RWS

Project name	Natte kunstwerken en trillingen
Project number	060.25718

Revision

Revision number	Date	Remarks
1.0	21 April 2017	Original
1.1	17 October 2017	• Comments based on Notes W. Kortlever 19 June 2017 and after discussions as summarized in email “Trillingenstudie, methode voor 'screening' van waterbouwkundige kunstwerken” dd. 5 September 2017.

Samenvatting

Voorwoord

Beschreven onderzoek in dit rapport wordt uitgevoerd in het kader van het Kennisplan Natte Kunstwerken 2017.
Het Kennisplan is de praktische concretisering van de NKWK[1]-onderzoekslijn 'Toekomstbestendige Natte Kunstwerken'. In deze onderzoekslijn werken momenteel Deltares, TNO, Marin, RWS en NLIngenieurs samen aan onderwerpen op het gebied van natte kunstwerken (stuwen, sluizen, gemalen en stormvloedkeringen).
Een groot deel van deze kunstwerken bereikt komende decennia einde technische levensduur. Er dient zich dan ook een aanzienlijke vervangings- en renovatieopgave van deze kunstwerken aan. Een opgave die niet alleen technisch van aard is, maar die ook rekening moet houden met het functioneren van het kunstwerk in het netwerk/systeem/regio.

In het Kennisplan Natte Kunstwerken wordt dan ook de benodigde kennis ontwikkeld langs 3 sporen:

- bestaand object	- inzicht in (einde) technische levensduur - levensduurverlenging
- object-systeem	- inzicht in (einde) functionele levensduur
- nieuw(e) object/objectonderdelen	- toepassen innovaties - inspelen op toekomstige ontwikkelingen.

Alle 3 de sporen dragen bij aan een effectief en efficiënte vervanging- en renovatieopgave en nieuwbouw van natte kunstwerken.

[1] Nationaal Kennisplatform Water en Klimaat

Aanleiding

Rijkswaterstaat (RWS) heeft in recente projecten een paar studies naar trillingen van sluizen gedaan of laten uitvoeren door Deltares. Hiervoor zijn de handboeken van Kolkman & Jongeling[2] (1) en Jongeling & Erdbrink[3] (2) gebruikt. Tijdens deze studies bleek dat het gebruik van de handboeken niet eenduidig was en er meerdere interpretaties van de gegevens mogelijk waren. Dit onderzoek vermindert de onzekerheid in de ontwerpfase (of renovatie fase) van een sluis of klep.

Onderzoeksvraag en -opzet (Ned.)

Het project dat bestond uit het uitvoeren van een literatuurstudie naar de gebruikt referenties en achterliggende originele referenties, had als doel het achterhalen van de onduidelijkheden en het beoordelen van de bruikbaarheid van de handboeken voor toekomstig gebruik.

Het gevolgde onderzoek bestond uit de volgende stappen:
- Interviews met Deltares en TNO betreffende de huidige gevolgde procedures en referenties.
- Literatuurstudie naar basis handboeken en naar originele referenties.
- Workshop met RWS, TNO en Deltares betreffende onduidelijkheden en gemis in huidige procedures en referenties.
- Verzamelen referenties & vormen aanbevelingen in welke referenties te volgen in basis ontwerp procedures.
- Rapportage

Onderzoek zelf

Een basis classificatie van trillingen kan worden opgesomd als:
- Stromings geïnduceerde excitatie
- Systeem (stroming en mechanica) geïnduceerde trillingen

In de eerste categorie (stromings geïnduceerde excitatie) reageert de mechanische structuur op de door de stroming geïnduceerde fluctuaties. Dit omvat turbulentie en excitatie door vortex shedding aan het object. Turbulente excitatie is vaak breedbandig (omvat veel frequenties) en de response van het lichaam is proportioneel aan de kinetische energy van de stroming (Figuur 1).

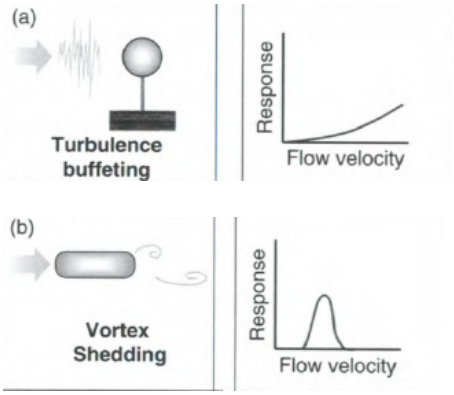

Figuur 1: Excitatie ten gevolge van turbulente fluctuaties en vortex shedding.

Bij de vortex shedding is er sprake van een opslingering in de amplitude van de trilling van het lichaam indien de mechanische eigenfrequentie en de vortex

[2] Dynamisch-gedrag-van-waterbouwkundige-constructies. Door B Kolkman & Jongeling deel A,B en C. (1996)
[3] Dynamica van beweegbare waterkeringen. Door Jongeling & Erdbrink. (2010)

shedding frequenties een veelvoud van elkaar zijn. Voor beide mechanismen (turbulentie en vortex shedding) geldt dat, indien de mechanische eigenfrequentie of vortex shedding frequentie overeenkomt met een akoestische/oppervlakte resonantie, de trillingsamplitude zal worden verstrek. De resonanties kunnen dan voorkomen als akoestische resonanties (in het waterdeel) of door resonantie in het water-lucht oppervlak. Het voorbeeld hierbij zijn staande watergolven in een sluis.

Daarom zijn er drie belangrijke bronnen die betrekking hebben op het eerste categorie:
- Turbulente (breedbandige) excitatie
- Akoestische/interface resonantie geïnduceerde excitatie. Dit zijn bevoordeeld excitaties door een staande watergolf in een waterbak.

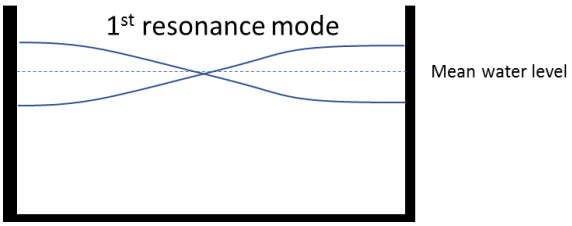

Figuur 2: Eerste resonantie mode van een wateroppervlak in een bak.

- Vortex shedding geinduceerde excitatie

In de tweede categorie (systeem (stroming en mechanica) geïnduceerde trillingen) vallen de mechanismes in welke de krachten op en het lichaam door de stroming en de mechanische trilling zelf gekoppeld zijn (Figuur 3).

Figuur 3: Excitatie ten gevolge van de koppeling van de bewegingen van het lichaam en de omhullende stroming.

Voor deze categorie geldt dat het systeem van het lichaam en de vloeistof eromheen samen instabiel worden. Deze instabiliteit kunnen gecategoriseerd worden door:
- Statische instabiliteit: De vloeistof resulteert in een extra negatieve stijfheid. Een voorbeeld hiervan is flutter.
- Dynamische instabiliteit: De vloeistof voegt negatieve damping toe. Een voorbeeld hiervan is galloping.

Voor de natte kunstwerken kunnen de trillingen in deze tweede categorie worden gekenmerkt door:
- Galloping : De krachten op de structuur in de verticale richting (de lift krachten) zijn afhankelijk van de stromingsrichting. (Figuur 4 a)
- Afsluiten (seals) : De weerstand over de afsluiting is afhankelijk van de bewegingssnelheid van de klep. (Figuur 4 b)

- Terugkoppeling : In combinatie met de traagheid van de stroming (stroomopwaarts of afwaarts) van de klep, zijn de lift krachten afhankelijk van de beweging van de klep. (Figuur 4 c)
- Dynamische loslating : Het loslaat punt van de stroming aan de klep is afhankelijk van de stand van de klep. (Figuur 4 d)

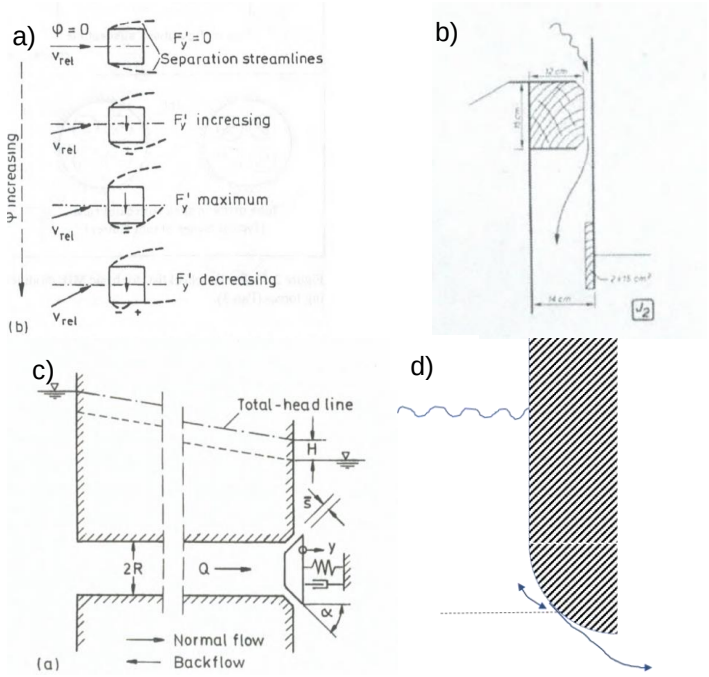

Figuur 4: Examples.

Een volledig overzicht van de meest voorkomende trilling excitatie mechanismen, met hun theoretische achtergrond en aanbevolen basis referenties zijn samen gezet in TNO rapport : TNO 2017 R10528.

Voor de evaluatie van de trillingen-potentie van een kunstwerk worden de volgende stappen aanbevolen:

1. Bereken de mechanische eigenfrequenties
2. Beoordeel de excitatie van horizontale trillingen (Criterion Naudascher)
3. Beoordeel de excitatie van verticale trillingen
4. Beoordeel onderdelen van de structuur die volledig in het water staan op vortex shedding en bepaal de shedding frequentie.
5. Beoordeel voor caviteiten en holtes die gevoelig zijn voor vortex shedding
6. Bereken de stroomopwaartse en stroomafwaartse resonantie frequenties voor zowel de akoestische als de water/lucht oppervlakte resonanties.
7. Beoordeel ontwerp voor galloping
8. Beoordeel ontwerp voor bewegingsgeinduceerde trillingen

Onderzoeksresultaten en synthese

Op basis van de handboeken en de oorspronkelijke referenties uit deze handboeken, zijn de huidige screening stappen verduidelijkt en uitgebreid. Veel aandacht is gegeven aan de het gebruik van de juiste definities zoals deze gebruikt zijn in de handboeken en de oorspronkelijke referenties.

Naast de huidige screening stappen zijn de volgende stappen toegevoegd (aanbevolen):

- Extra screenen voor trillingen in de horizontale richting voor sluizen en kleppen. Dit is vooral van belang voor lichtere constructies. Zeker daar in de toekomst lichtere materialen (kunststoffen) zullen worden gebruikt, is dit een belangrijke nieuwe excitatie mode.
- De screening voor trillingen in de verticale richtingen van sluizen en kleppen is uitgebreid zodat nog beter deze excitatie mode kan worden uitgesloten.
- De screening voor de galloping mode voor sluizen en kleppen met onderstroming is uitgebreid.

Een volledig overzicht van de meest voorkomende trilling excitatie mechanismen, met hun theoretische achtergrond en aanbevolen basis referenties zijn samen gezet in TNO rapport : TNO 2017 R10528.

Evaluatie en vooruitblik

Naar aanleiding van het onderzoek en het rapport worden de volgende aanbevelingen gedaan:

- Uitbreiding screening naar excitatie horizontale trillingen in sluizen en kleppen.
- Uitbreiding screening voor de excitatie van verticale trillingen in sluizen en kleppen
- Uitbreiding screening voor de excitatie van de galloping mode in sluizen en kleppen
- Vergelijk van huidige ontwerp regels met ontwerp aanbevelingen van buitenlandse nationale instituten.
- Het uitvoeren van CFD simulaties aan het basis ontwerp van sluizen/kleppen om de weerstand en lift coëfficiënten te bepalen.
- Het uitvoeren van CFD simulaties voor gebruik in afschatting van bewegings-geïnduceerde instabiliteit.

Contents

1 Introduction

1.1 Introduction

This report forms part of the deliverables for project 060.25718, which is a TNO assignment by RWS. The goal of the project is to review currently used screening methodologies and input as used by RWS and Deltares for screening purposes of designs of gates and valves. The first main deliverable was a workshop as held at TNO (Delft) on 24 Jan 2017. This report forms the second main deliverable.

1.2 Report goals

The goal of the report is to give an overview of the main excitation mechanisms for vibrations of valves and hydraulic gates. Of course, in a limited report it is impossible to give a complete overview. The number of scenarios and different designs is that large that not a complete overview can be written. However, the background serves as input for the screening steps for evaluating the likelihood of vibrations of gates and valves.

1.3 Report structure

The report is setup that in Chapter 2 a discussion is given regarding the classification of flow induced vibrations. A theoretical background and introduction of the main mechanisms are given in Chapter 3. The main chapter is Chapter 4 in which the screening steps and required reference figures are discussed. Chapter 5 covers a discussion of a specific topic of sealing. Finally in Chapter 6, an overview is given of recommendations and lessons learned from the main literature references. The report closes with recommendations and a full bibliography list. In the annexes, most of the background figures are added for easy reference.

1.4 References

In this report, a lot of references are used to specific pages (to help in finding the original references). The following reference abbreviations are used:

K&J Kolkman & Jongeling, “Dynamisch gedrag van waterbouwkundige constructies”, Dutch version (Kolkman & Jongeling, Dynamisch gedrag van waterbouwkundige constructures (deel A, B en C), 1996)

N&R Naudascher and Rockwell, Flow induced vibrations, An engineering guide”, 1994 (Naudasher & Rockwell, Flow-Induced Vibrations, 1994)

Nau Naudasher, “Hydrodynamic Forces” IAHR series”, 1991 (Naudasher, Hydrodynamic forces, 1991)

Blevins Blevins, “Flow-induced Vibration. Second edition”, 2001 (Blevins, 2001)

Kaneko Kaneko, et.al, Flow induced vibrations, Classifications and lessons from practical experiences”, English version, 2008 (Kaneko, Nakamura, Inada, & Kato, 2008)

For other literature the normal references are used.

2 Classification

2.1 Introduction

Different authors classify the excitation and vibration mechanisms in different ways. In the end all mechanisms are covered but the different classifications are useful in the sense of different viewpoints and different starting points in evaluating and screening a design.

In Annex A, different classifications are covered by:

- Kaneko (Kaneko, Nakamura, Inada, & Kato, 2008)
- Naudascher (Naudasher, Hydrodynamic forces, 1991)
- Kolkman & Jongeling (Kolkman & Jongeling, Dynamisch gedrag van waterbouwkundige constructures (deel A, B en C), 1996)
- Erdbrink (Erdbrink, Modelling flow-induced vibrations of gates in hydraulic structures, 2014)

2.2 General classification

The most basic classification which can be made is :

- Flow-Induced excitation
- Fluid-Structure interactions

In the first excitation mechanism (flow-induced excitation), the mechanical structure responses to fluid forces. These include broadband excitations such as turbulence in which the response is proportional to the turbulent fluctuations. In general the response (A) is proportional to the kinetic energy of the flow A ~ρU^2 (Figure 1)

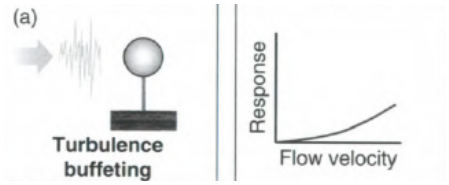

Figure 1: Excitation due to turbulent buffeting.

The second excitation type which falls within this first mechanism (flow-induced excitation) is vortex shedding induced excitation (Figure 2).

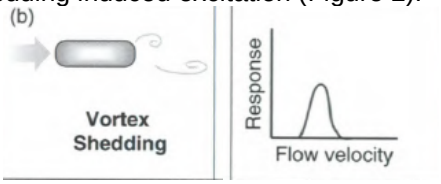

Figure 2: Excitation due to vortex shedding.

The structure responses to vortices shed on the body. These result in fluctuating forces on the body. If the vortex shedding frequency (or multiples thereof) coincides with the mechanical natural frequency, large vibrations can occur.

Both of the excitation mechanism are enhanced if the shedding or mechanical resonance frequencies coincide with any acoustic or interface (water-air) resonance. Such a resonance will synchronize and strengthen the vortex shedding. These resonances will result in a varying pressure and therefore a varying force on the structure. An additional effect is that the fluctuating pressure field will enhance the instabilities encountered in the vortex shedding. Therefore, the forces on the body will increase. A similar effect occurs if the body itself is vibrating. This will enhance the vortex shedding and potentially also force the vortex shedding occurring at the vibration frequency. A classic example of this is the coincidence of vortex shedding and an acoustic resonance. In case the acoustic resonance frequency coincides with the vortex shedding frequency the amplitude of the lift forces is 6-10 times higher than if there is no such coincidence.

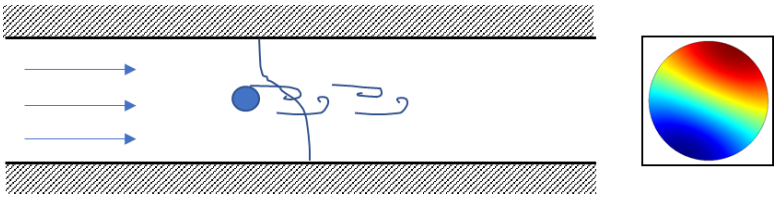

Figure 3: Example of combination vortex shedding and acoustic resonance with on the left side view and on the right the first acoustic transversal mode.

Therefore in the first category (flow-induced excitation) three important sources can be distinguished:

- **Turbulent broadband excitation**
- **Acoustic/resonance induced excitation**
- **Vortex shedding (shear layer instabilities which is a narrow band excitation)**

In the second category (fluid-structure interaction), mechanisms fall in which the fluid forcing and the body vibrations are coupled (Figure 4). To some extent this occurs in the feedback of the vortex shedding in a vibrating body.

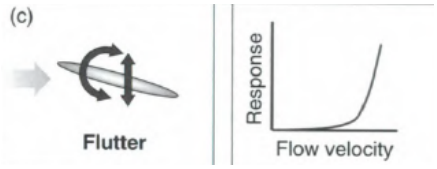

Figure 4: Excitation due to coupling between vibrating body and surrounding fluid.

For this mechanism, it can be stated that the full system of body and surrounding fluid becomes instable. These instabilities can be divided into two categories:

- Static instability (negative fluid stiffness larger than positive mechanical stiffness). An example is wing stall flutter
- Dynamic instability (negative fluid damping is larger than positive mechanical damping). An example is galloping.

With respect to the gates we can make a subdivision in self-excited vibrations:

- **Galloping: The lift coefficient is dependent on the inclination angle This can often be evaluated based on steady state calculations (Figure 5 a)**
- **Sealing: The sealing is dependent on the velocity of gate (Figure 5 b)**
- **Feedback: Feedback of dynamic lift forces due to movement coupling with acceleration of (up/downstream) fluid (Figure 5 c)**
- **Dynamic separation: The flow separation depends on the flow and/or structure velocity (Figure 5 d)**

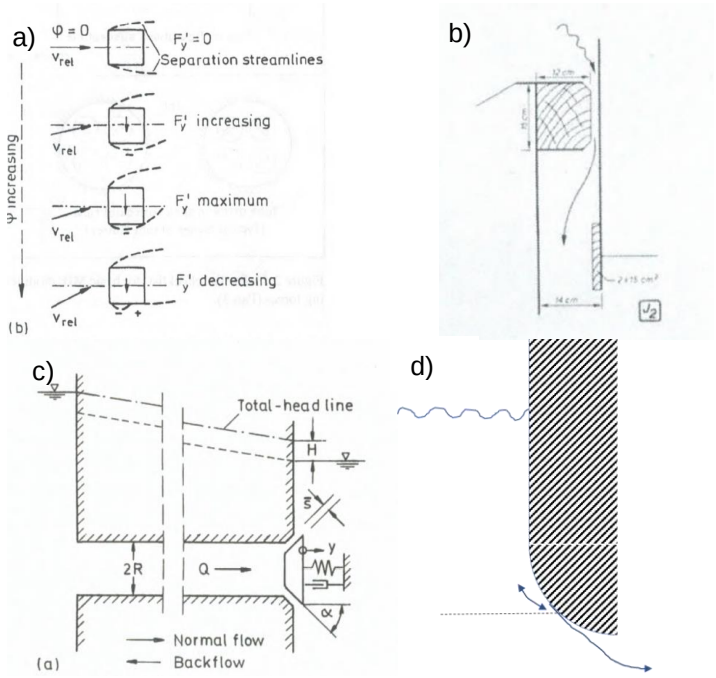

Figure 5: Examples.

In the next chapter, each of these mechanisms will be discussed to give a short theoretical background.

3 Mechanism

3.1 Turbulence

3.1.1 Discussion

In most scenarios, the flow surrounding the gates and valves is turbulent. That means that there are velocity and pressure fluctuations in the flow. These fluctuations are in general broadband with respect to the frequency content. The amplitude of the velocity fluctuations is typically 10% of the main stream velocity. That means that typical pressure fluctuations are $p' = 0.01 \cdot \frac{1}{2}\rho U^2$ [Pa]. This covers the complete frequency range.

3.2 Vortex shedding

3.2.1 Discussion

A shear layer is formed when the boundary layer on a body separates from the wall. This shear layer forms a velocity gradient. This velocity gradient can 'roll-up' into a vortex. This shear layer instability has two results:

- The first aspect is that it acts as an amplifier/attenuator for pressure disturbances (Figure 6). That is, a pressure disturbance is amplified (or damped out) by the shear layer instability. This is important in the coupling of acoustics and the shear layer. At a cavity or T-joint any acoustic wave can be amplified and can result in case of a resonance in a tonal sound generation. In practical terms: the shear layer can act as an acoustic source.
- The second aspect is that the vortices result in a fluctuating pressure at the body and therefore fluctuating forces on the body.

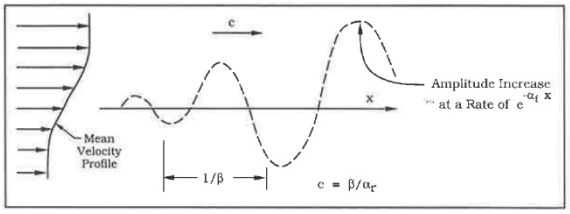

Figure 6: Amplification of a shear layer.

Typical examples of shear layer instabilities are given in Figure 7.

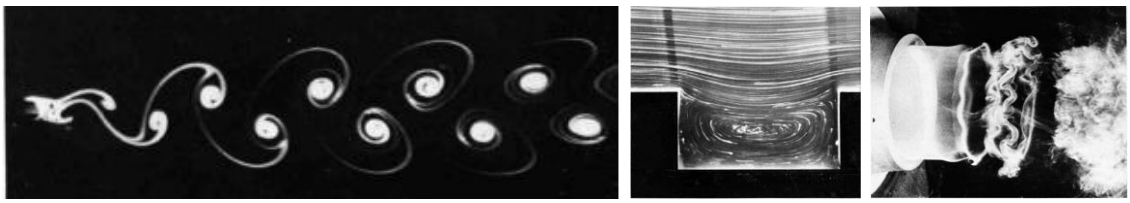

Figure 7: Typical shear layer instabilities: bluff body, cavity and (circular) jet.

The vortex shedding frequency (*f*) is in general expressed as a dimensionless Strouhal number (*Sr*) defined via:

$$Sr = \frac{f\,D}{U}$$

In this equation, *U* is in general the upstream velocity [m/s] and *D* the characteristic length scale. In principle, *U* is the convective velocity of the disturbances (vortices) and *D* the effective path length which the vortices travel. This is the easiest seen for the typical Strouhal number of a cavity (Figure 8). The shear layer connects a zone with the mainstream velocity and a zero velocity. The typical velocity of the disturbance will be approximately half the main velocity and the path length is the gap width. This would lead to a Strouhal number of Sr ~ 0.5.

For a deep cavity the Strouhal is given by:

$$Sr = \frac{n - \xi}{1 + 1/k_v}$$

with n=1, 2, 3, .. , ξ = 0.25 and k_v the convection velocity of k_v = 0.57. This would lead to a first mode of Sr = 0.3 (with additional modes at 0.6, 1).

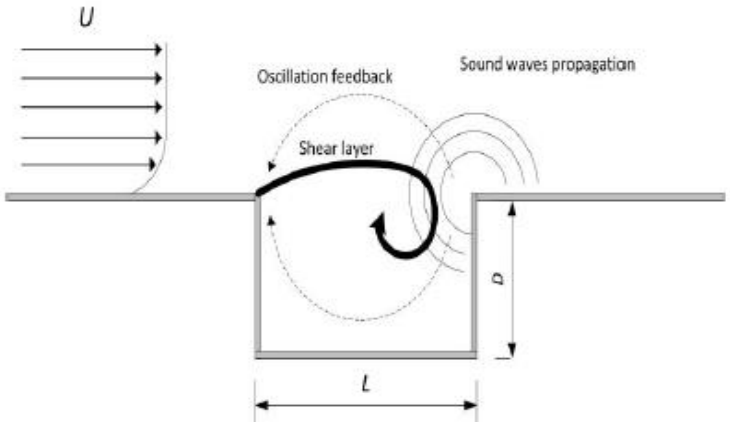

Figure 8: Vortex shedding at a cavity.

For bluff bodies (2D structures) typical Strouhal numbers are Sr = 0.2 with the effective length the thickness of the body.

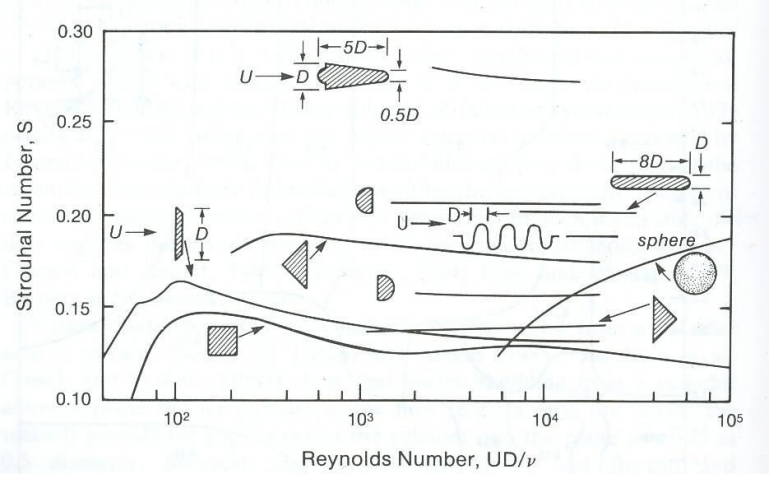

Figure 9: Strouhal number of bluff bodies (Blevins, 2001).

Important considerations are:

- Each geometry has its own Strouhal number.
- As the Strouhal number is dependent on the convection velocity and the effective path length, the details of the flow are important. The details of the geometry and the boundary layer thickness determine the velocity gradient in the shear layer and therefore the convection velocity and path length. Therefore, the Strouhal number is dependent on the Reynolds number (*Re*). However, for large variations of Reynolds number the Strouhal number is approximately constant.
- Often the measurements are done in free field conditions. Therefore the reference velocity is often taken as the upstream conditions. However, if the body is for instance placed in a confinement, the velocity at the top of the shear layer should be taken as reference.
- The vortex shedding results in a fluctuating force on the body. The lift force has the same frequency as the vortex shedding. The force in the drag direction has DOUBLE the vortex shedding frequency.

3.2.2 Examples – cylinder

The most classic but also the most complex example is the flow around a cylinder. It is the most complex as the separation point on the body is strongly dependent on the Reynolds number. This separation point determines the effective velocity gradient and the effective spacing between the two shear layers. As the opposing shear layer influences the velocity of the other shear layer, the change in separation will influence the Strouhal number.

In Figure 10 the Strouhal number as function of Reynolds number is given. The Reynolds number is based on the cylinder diameter.

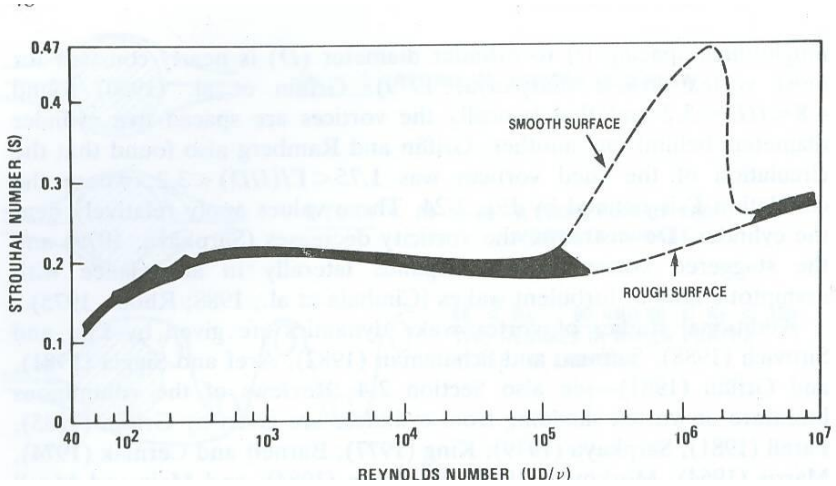

Figure 10: Strouhal number as function of Reynolds number (Blevins, 2001).

3.2.3 Example – plates

The Strouhal number for plates is very dependent on :

- Edge rounding
- Length/width ratio
- Angle (of attack)

The edge rounding is important similar to the discussion on the cylinder. Where exactly the separation occurs is important.

The other two parameters are important as in plates two separation areas are present: at the upstream edge and at the downstream edge. The length/width ratio is important in determining which is dominant. Furthermore, vortices formed at the upstream edge which are entrained along the plate might result in fluctuating forces on the plate.

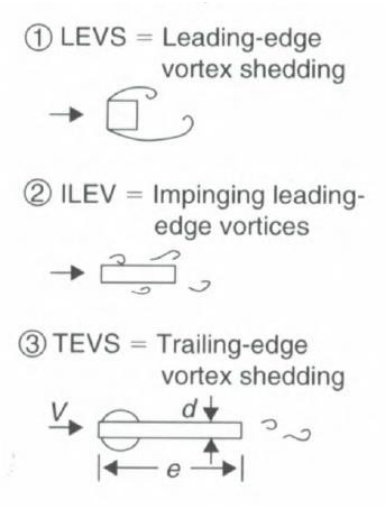

Figure 11: Leading egde vs trailing edge separation (Kaneko, Nakamura, Inada, & Kato, 2008).

At zero inclination, the effective length scale is the plate thickness and the Strouhal number based on the plate thickness is Sr ≈ 0.2 (see for details Annex D.3). However at 90 degree inclination, the effective length should be the plate length. This is also clear from Figure 12 in which the Strouhal number is plotted for a plate at different angles.

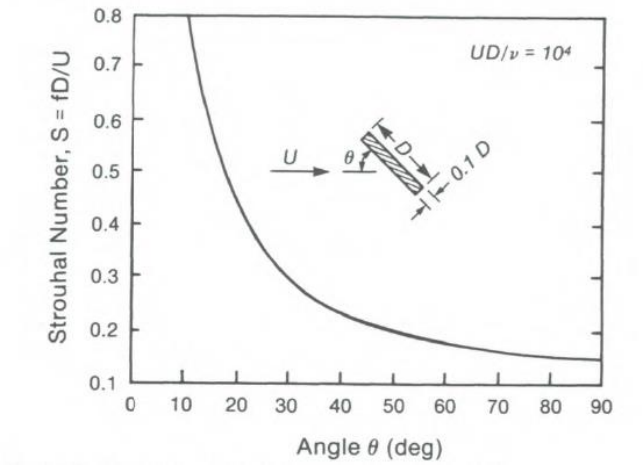

Figure 12: Strouhal number as function of inclination (Blevins, 2001).

In Annex D.3 the Strouhal number is given as function of plate aspect ratio, edge rounding and angle.

3.2.4 Example – orifices

The orifices are covered because they are very insightful in showing the difference between vortex shedding on a sharp edge vs vortex shedding on a thick structure.

For sharp edged structures, the separation point is fixed and the main instability is a jet instability (Figure 13). The typical Strouhal number associated with that is

$Sr = fD/U = 0.2$

With D the jet diameter and U the jet velocity.

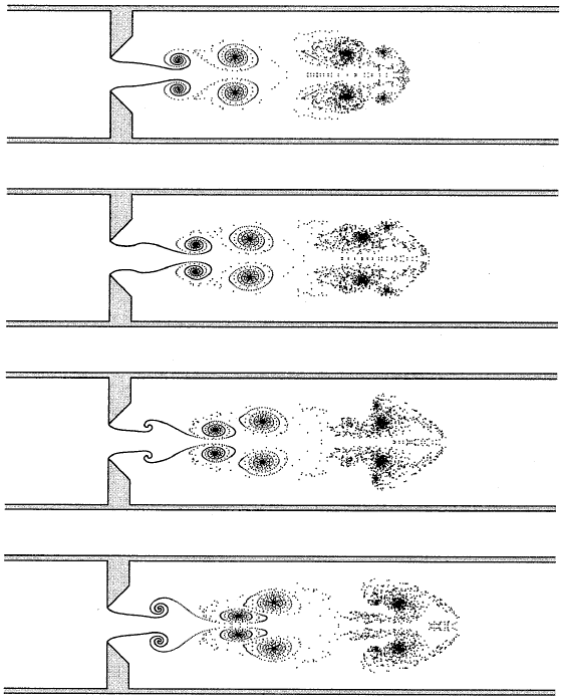

Figure 13: Jet formation on a sharp orifice.

However, at thicker orifices the boundary layer separates at the upstream edge and the instability ‘travels’ from the upstream to the downstream edge. In that case the thickness of the plate is the relevant length scale (Figure 14).

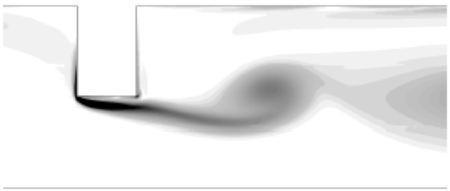

Figure 14: Vortex shedding on a thick orifice.

In that case the bevelling of such a plate can have a huge impact. As a downstream bevelling ‘just’ results in a thinner orifice. An upstream bevelling can result in more jet like instability (more broadband noise).

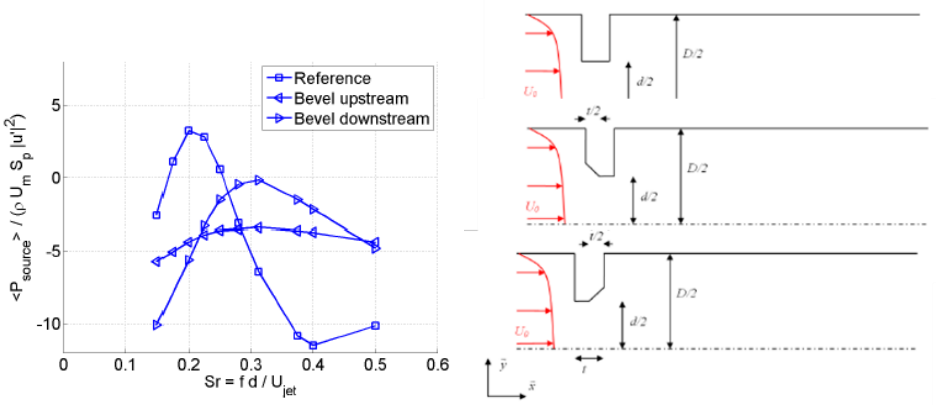

Figure 15: Influence of upstream or downstream bevelling. Left figure shows generated source power as function of Strouhal number for a selection of geometries (right figure). A positive power means positive generation of sound; negative power means absorption.

For completeness the Strouhal number for a thick orifice is given by (Testud, Aurgean, Moussou, & Hirschberg, 2009):

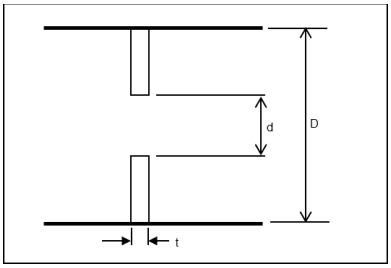

$$Sr = 0.2420\left(1+\frac{31.69}{\sqrt{\mathrm{Re}}}-.0657\frac{D}{D-d}\right), \quad \text{for } \mathrm{Re} \geq 5000$$

3.3 Broadband noise

3.3.1 Bends and valves

Broadband sources, as for example valves and bends are added for completeness. These are less relevant for the hydraulic gates but might be important in more closed in systems like sluice gates and sewer drainage with valves. If sharp bends are present close by a valve/gate, the fluctuations generated by the bend will lead to an increased turbulent ‘buffeting’ to the valve.

Bends and orifices will generate a high amplitude broadband noise spectrum (Violato, De Jong, & Golliard, 2016). Estimations are possible based on the pressure drop across the device and steady state (CFD) simulations. Based on a ‘universal’ scaled power spectrum a translation can be made for a specific configuration. The scaling is not reproduced here but can be found in (Violato, De Jong, & Golliard, 2016). As stated, this is mainly important for closed in systems with sharp bends or with bends with high flow rates.

3.4 Self-excited vibrations

In this section a number of motion induced vibration mechanisms are discussed.

3.4.1 Dynamic instability (N&R p 56)

The dynamic stability is related to the presence of an added damping term. For example a cylinder in cross flow has the load (per unit length) of:

$$F_y(t) = \rho d^2 \omega_n (\omega_n h_a y + k_a \dot{y})$$

with ω_n the natural frequency, h_a the added mass coefficient and k_a the excitation coefficient. This excitation coefficient is proportional to the velocity and as such can be considered as a damping term. The full equation of motion for this case can be written as:

$$m_r \ddot{\eta} + (Sc - k_a)\dot{\eta} + (m_r - h_a)\eta = 0$$

in which $\eta = y/d$; $m_r = m/(\rho d^2)$ and

$$Sc = 2\frac{m}{\rho d^2}\xi$$

The stability criterion is in that case simply:

$$Sc - k_a > 0$$

Thus, for those cases that the excitation term is proportional to the velocity of the body, a dynamic instability can occur.

A less complicated example is by leaving out the mass term in the excitation (Nau 65). A prism/object is subjected to a cross flow leading to lift forces (Figure 16).

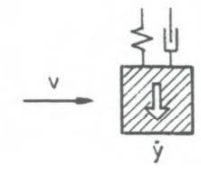

Figure 16: Body in cross flow.

The equation of motion for the body is:
$m\ddot{y} + 2m\zeta\omega_n\dot{y} + m\omega_n^2 y = F_y$

The force is given by:
$F_y = C_y d \frac{1}{2} \rho v^2$

with C_y the lift coefficient. The lift coefficient can be written as a series dependent on the inclination angle which is proportional to the velocity of the body.

$$C_y = \sum_{j=1}^{n} a_j \left(\frac{\dot{y}}{v}\right)^j$$

This leads to the equation of motion:

$$m\ddot{y} + 2m\zeta\omega_n\dot{y} + m\omega_n^2 y = F_y = d\tfrac{1}{2}\,\rho v^2 C_y = d\tfrac{1}{2}\,\rho v^2\ \sum_{j=1}^{n} a_j \left(\frac{\dot{y}}{v}\right)^j$$

$$\ddot{y} + \left(2\zeta\omega_n - \tfrac{1}{2}\frac{\rho v d}{2m}a_1\right)\dot{y} + \omega_n^2 y = d\tfrac{1}{2}\,\rho v^2\ \sum_{j=2}^{n} a_j \left(\frac{\dot{y}}{v}\right)^j$$

At small $\dot{y}$ the right hand side is zero and the stability criterion is given by:

$$2\zeta\omega_n - \frac{1}{2}\frac{\rho v d}{2m}a_1 = 0$$

The critical aspect is that due to the movement a force occurs which is in phase with the velocity and therefore can be imagined as a damping term.

3.4.2 Static instability (N&R p 62)

The static instability is related to the stiffness term (rather than the damping term in the dynamic instability case). In this section the discussion of N&R (p62) is followed. If a linear displacement produces a force (or moment) which tends to increase the displacement, static instability can occur. Static instability requires negative stiffness in excess of the positive mechanical stiffness. The force is in this scenario in phase with the displacement or with the acceleration.

Considering the gate in Figure 17, the fluid force in case of small vibrations is given by:

$$F_y = \frac{1}{2}\rho V^2 D\left[C_{ye} + \left(\frac{dC_y}{dy}\right)_e y\right]$$

The subscript *e* denotes that this is at equilibrium and C_y the lift coefficient.

For static equilibrium it holds that

$$Cy = F_y$$

With C the (mechanical) spring stiffness. This results in:

$$\left[C - \frac{1}{2}\rho V^2 D\ \left(\frac{dC_y}{dy}\right)_e\right] y = \frac{1}{2}\rho V^2 D C_{ye}$$

The displacement will become infinite if the total stiffness (between the square brackets) becomes negative. This leads to a critical velocity of

$$V_{crit} = \sqrt{\frac{2C}{\rho D\left(dC_y/dy\right)_e}} = \omega_n D\sqrt{\frac{2m/(\rho D^2)}{D\left(dC_y/dy\right)_e}}$$

with

$$\omega_n = \sqrt{\frac{C}{m}}$$

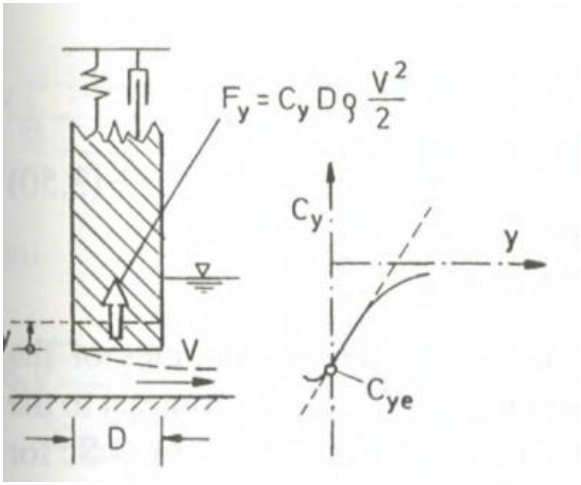

Figure 17: Gate with a submerged underflow (Nau p63).

The negative fluid stiffness is a base example of the plug flow. The negative stiffness can occur due to the large inertia of the flow. The example given by N&R is a good example (Figure 18).

The plug is an example of Kolkman (Kolkman, Flow-induced gate vibrations. , 1976). Due to the large momentum of the flow, the flow Q will not change due to fluctuations *y* of the valve. The head (*H*) across the valve can be described as:

$$H = (Q/(sb))\text{^}2\ /2g$$

with *b* the circumference of the gap [m] and *s* the gap width [m]. This head has an average and time dependent part as:

$$H = \bar{H} + H(t) = \bar{H}\left(\frac{\bar{s}}{\bar{s} + y sin\alpha}\right)^2 \cong \bar{H}\left(1 - \frac{2\sin\alpha}{\bar{s}}y\right)$$

The force on the plug is given by

$$F_y \cong \rho g H A_v \cong \frac{1}{2}\rho\frac{A_v}{(\bar{s}b)^2}\bar{Q}^2\left(1 - \frac{2sin\alpha}{\bar{s}}y\right)$$

This force can be considered as a negative stiffness (force is proportional to the displacement) and therefore this system can become unstable.

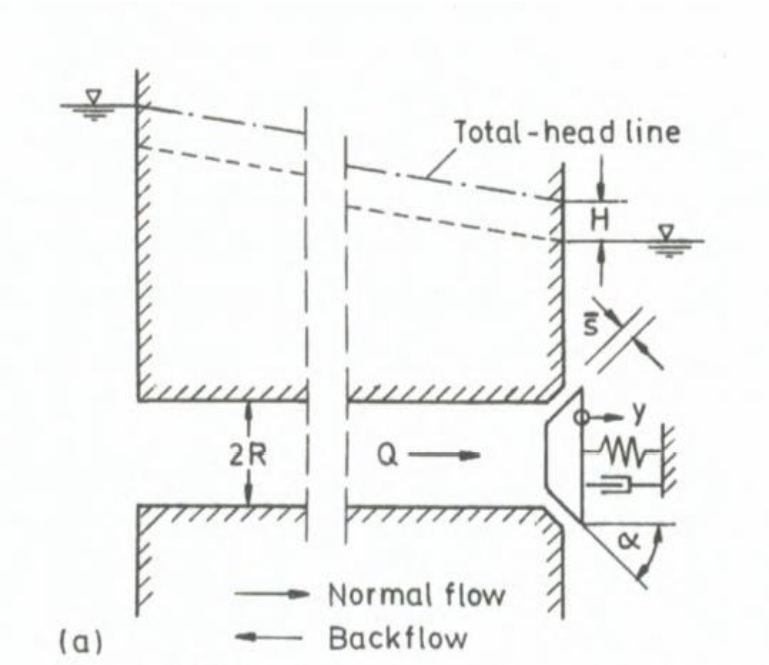

Figure 18: Example of static instability (N&R p 64).

3.4.2.1 Galloping

In case of vortex shedding without re-attachment, movement-induced excitation occurs without a phase shift between fluid force and instantaneous body velocity (N&R p 200). This occurs for short bluff bodies and for gates with underflow.

Short bluff bodies is the classic example given for galloping (Nau p 64 – 65) . If a prism is vibrating the velocity of the body can be considered as a change in the effective flow direction. The angle is

$$\varphi = \tan^{-1}\frac{\dot{y}}{v}$$

The fluid-dynamic force (lift direction) is given by:

$$F_y' = \frac{1}{2} C_y \rho d\, v^2$$

The equation of motion for the body is given by:

$$m\ddot{y} + 2m\xi\omega_n\dot{y} + m\omega_n^2 y = \frac{1}{2} C_y \rho d\, v^2$$

If a quasi-steady approach is used the lift coefficient can be developed into:

$$C_y = \sum_j^n a_j \left(\frac{\dot{y}}{v}\right)^j$$

If the first order term is included into the main equation of motion:

$$\ddot{y} + \left(2\xi\omega_n - \frac{\rho v\, d}{2m} a_1\right)\dot{y} + \omega_n y = \frac{1}{2}\frac{1}{m}\rho d v^2 \sum_{j=2}^{n} a_j \left(\frac{\dot{y}}{v}\right)^j$$

The stability criterion is in that case that the total damping must be larger than zero. This is always the case if a_1 is smaller than zero. This gives a critical velocity of:

$$V_r = \frac{v}{f_n d} < \frac{4\pi}{a_1} Sc$$

with

$a_1 = \frac{dC_y}{d\alpha}$ and $Sc = \frac{2m\xi}{\rho d^2}$

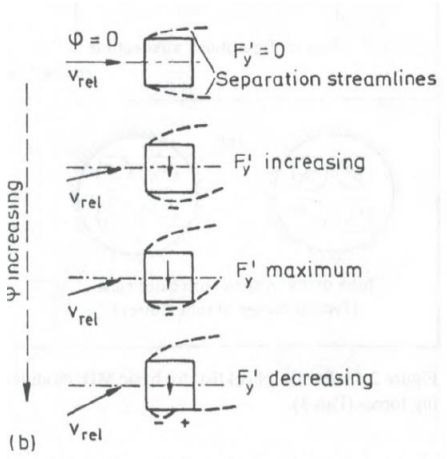

Figure 19: Vibrating prisms (Nau p 64).

Other similar derivations can be found in most text books. Another example is Blevins p 106 (Figure 20).

$$\alpha = \arctan\left(\frac{\dot{y}}{U}\right)$$

$$U_{rel}^2 = \dot{y}^2 + U^2$$

$$F_y = -F_L cos\alpha - F_D sin\alpha = \frac{1}{2}\rho U^2 D\, C_y$$

$$C_y = -\frac{U_{rel}^2}{U^2}(C_l cos\alpha + C_d sin\alpha)$$

The lift coefficient is again expanded in power series (small angles)

$$C_y(\alpha) = -C_L|_{\alpha=0} - \left[\frac{\partial C_L}{\partial \alpha} + C_D\right]\alpha + O(\alpha^2)$$

This leads to the similar equation of motion

$$m\ddot{y} + 2m\xi\omega_n\dot{y} + ky = \frac{1}{2}C_y\rho D\, U^2$$

$$m\ddot{y} + 2m\omega_n\left(\zeta - \frac{\rho UD}{4m\omega}\frac{\partial C_y}{\partial \alpha}|_{\alpha=0}\right)\dot{y} + ky = -\frac{1}{2}\rho D\, U^2 C_L|_{\alpha=0}$$

This is always stable if:

$\frac{\partial C_y}{\partial \alpha} < 0$ or $\frac{\partial C_L}{\partial \alpha} + C_D > 0$

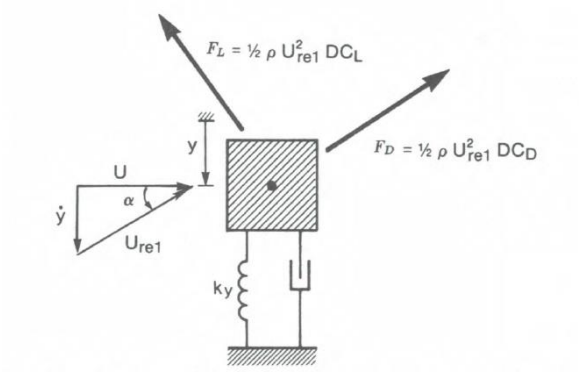

Figure 20: Galloping definitions (Blevins p 106).

For <u>gates with underflow</u> Naudascher (Nau p 208) argues a similar analysis to the galloping analysis. His statement is that: "*Where the C_L versus s/e curves exhibit a positive slope, there is danger of soft excitation due to galloping unless either Sc is larger than a critical value or the maximum V_r is smaller than $V_{r,crit}$. Where these curves have zero slope, hard galloping (or movement induced excitation involving inertia coupling) is possible.*"

The example is given in Figure 21. The conditions with $\partial C_L/\partial(s/e) > 0$ show vibration.

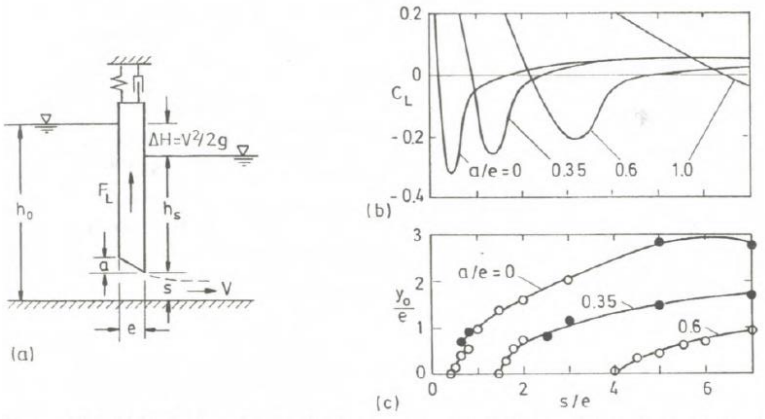

Figure 21: Example (Figure 7.27 N&R p 209)

In this C_L is the lift coefficient, *s* the gap width and *e* gate width.
Note: the inertia coupling is the 'plug' flow.

Naudascher argues that movement induced vibration is a mixture of

a) Galloping
b) Excitation involving inertia coupling with fluid-flow pulsations.

3.4.3 'bath plug'

The plug model is discussed as it is a main part in the screening as used by RWS.

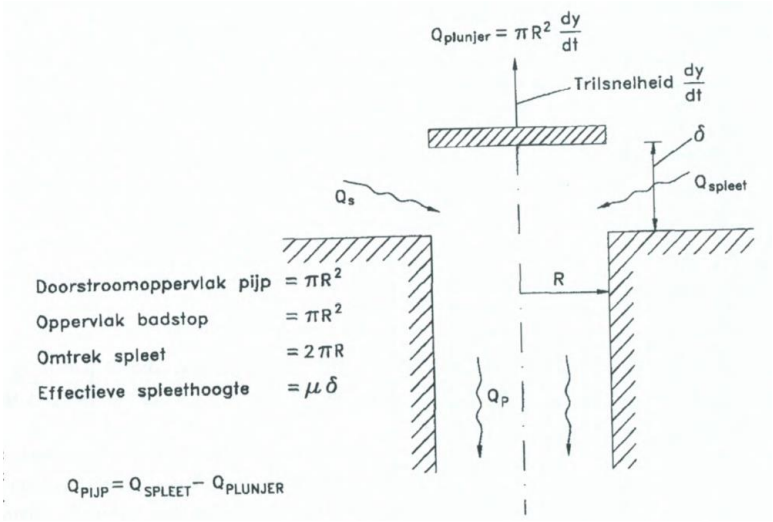

Figure 22: Definitions for 'bath plug' analysis (K&J p 94).

In the analysis as presented by Kolkman (K&J p 94) the following steps are critical:

- The volume flux is dependent on the movement of the plug
- The mass downstream of the plug is 'short' such that it can be considered as a single mass. That means it can be considered incompressible. This is true as long as the first acoustic resonance in that line is higher than the valve resonance frequency.

The first step leads to an equation in which the change in velocity in the downstream channel is coupled to the movement of the plug. If this relation is linearized such that only small variations are considered.

$$Q_{pipe} = Q_{slit} - A_{plug}\frac{dy}{dt}$$

With the slit velocity as

$$Q_{slit} = A_{slit}\sqrt{2g\Delta H}$$

In this the slit area is given by $A_{slit} = \delta\mu(2\pi R)$
This in total leads to (K&J equation A4.14):

$$\frac{dV'}{dt} = \frac{2\mu}{R}\sqrt{2g\Delta H_0}\frac{dy}{dt} + \frac{\mu\delta_0}{R}\sqrt{\frac{2g}{\Delta H_0}}\frac{d\Delta H'}{dt} - \frac{d^2y}{dt^2}$$

The change in head across the plug and the flow velocity fluctuations are coupled due to the inertia in the downstream pipe:

$$\Delta H' = -\frac{L}{g}\frac{dV'}{dt}$$

This last equation comes from

$$F' = ma$$

$$\rho g\, \Delta H' A_{pipe} = \rho L\, A_{pipe} \frac{dV'}{dt}$$

This can be used in the equation A4.14 and will lead to an equation as:

$$\alpha \frac{d^3y}{dt^3} + \beta \frac{d^2y}{dt^2} + \gamma \frac{dy}{dt} + \delta y = 0$$

Assuming a harmonic oscillation, this leads to a stability criterion of:

$$C_k > 1 + C_m$$

with

$C_m = \frac{m}{\rho A_{pipe} L}$; $C_k = \frac{k\delta_0}{2\rho g\, \Delta H_0 A_{pipe}}$

(Note that in the lengths and masses correction for added mass and added lengths are included).

4 Screening

4.1 Introduction

In this chapter, the different screening steps are discussed. As with the classification, different steps and different flavours are possible. Different flavours of screening can be found in the literature:

- Kolkman and Jongeling (book C, p13)
- RWS
- Naudascher
- Erdbrink

These are described in Annex B.

In this chapter, a basic screening is used which is a mixture of these. This procedure is followed step by step and the most important graphs and figures are discussed. The aim of this discussion is to find which graphs and scenarios are not fully described.

4.2 Screening steps

The common steps between the different procedures are

1. Calculate mechanical eigenfrequencies and eigenmodes
2. Calculate potential fluid resonances (in the fluid (acoustic) and interface waves)
3. Calculate turbulence induced excitation
4. Calculate vortex shedding frequencies
    a. Behind the main gate
    b. Below the gate
5. Compare mechanical, resonance and excitation frequencies.
6. Evaluate galloping mechanism
7. Evaluate potential changing discharge coefficient
8. Evaluate potential changing non-constant separation points
9. Evaluate momentum upstream & downstream of valve (‘bath plug’ mechanism)

4.3 Criteria

4.3.1 Vortex shedding

For systems with vortex shedding to completely avoid any interaction between the vortex shedding and the mechanical vibration the following rules are found:

JSME Guidelines (Kaneko p39)

The JSME S012 (turbulent excitation) code prescribes for a single cylinder:
$V_r < 1$ for complete avoidance
$V_r < 3.3$ avoidance of lift oscillations (for this also the damping must be C_n>2.5)

with

$$V_r = \frac{V}{f_0 D}$$

with *V* the upstream velocity [m/s], f_0 the mechanical eigenfrequency [Hz] and *D* the cylinder diameter.

The damping parameter is defined via:

$$C_n = \frac{4\,\pi m\,\xi}{\rho D^2}$$

with ρ the fluid density [kg/m3] and ξ the damping ratio.

At a typical Strouhal number of Sr = 0.2, this gives a limit of the ratio f(vortex)/f(mechanical) of

$\frac{f_{vortex}}{f_{mechanical}} = 0.66$ for avoiding coincidence in the lift direction or a safety factor of 1.5

$\frac{f_{vortex}}{f_{mechanical}} = 0.2$ for avoiding coincidence in the drag direction or a safety factor of 5

ASME Guidelines

The ASME Code sec III, Div. 1, Appendix N, 1300 series has the same limits as the JSME code for avoidance but also adds a stricter limit for the damping (C_n>1.2).

For avoidance of lift oscillations a margin of 30% is allowed:

$$\frac{f_0}{f_w} < 0.7 \;\&\; \frac{f_0}{f_w} > 1.3$$

In this f_0 is the mechanical eigenfrequency and f_w is the vortex shedding frequency.

AVIFF guidelines

The AVIFF prescribes a margin of 20% for vortex shedding on thermowells. This means no oscillations in the drag direction are considered.

Kolkman & Jongeling

Kolkman & Jongeling recommend a safety factor of 2-3 between the vortex shedding frequency and the mechanical eigenfrequency.

Please note that this is a very safe factor in case of 'single' vortex shedding (shedding beneath a valve). In case of for instance a cylinder this is less safe. The excitation frequency in the axial direction (in the drag direction) is double the vortex shedding frequency. The excitation frequency direction in the lift direction (perpendicular to the flow) is the vortex shedding frequency. With a margin of 2-3, the lift direction has a margin of 2-3, but in the drag direction the margin is 1 – 1.5. This is not a safe margin.

4.4 Screening calculation steps (input and discussion)

4.4.1 Calculate mechanical eigenfrequencies and eigenmodes

Determine the lowest mechanical eigenmodes and eigenfrequencies. It is important that the correct added mass and stiffness coefficients are used. Please note that these coefficients may depend on the position of the valve.

A more detailed discussion on this topic falls outside the scope of this report. Some remarks are made in the Annex F.

4.4.2 Calculate potential fluid resonances (in the fluid (acoustic) and interface waves)

In the vicinity of the object of interest fluid resonances can occur. These can be divided into two categories: One associated with the gas-liquid interface and one which occurs in the fluid itself (these are compressibility dominated and are also called acoustic resonances). It must be noted that the acoustic resonances can also have a gas-liquid interface as boundary. Examples of the most common resonators are given in Figure 23.

Good overviews of the resonance modes can be found in:

- Kolkman & Jongeling chapter 2.3 (K&J A p47 – 56)
- Naudascher section 2.2.4 (Nau)
- Naudasher and Rockwell Chapter 4 (p 67 – 90) (N&R)

The critical parameter in resonances are

- The acoustic (fluid) speed of sound
- The dimensions of the system
- The wave speed of interface waves

The speed of sound (c_a) for a fluid is given by:

$$c_a = \sqrt{\frac{E}{\rho_{fluid}}}$$

with

E Fluid bulk modulus [Pa]

For water the salt content also plays a role in the speed of sound. For water a typical speed of sound is *c* = 1400 – 1450 m/s.

The speed of sound for a gas is described by:

$$c_a = \sqrt{\kappa R T}$$

with

κ Isentropic coefficient [-]
R Specific gas constant (for air R = 287 J/(kg K)
T absolute temperature [K] (273.15 + T [°C])

The wave speed for gas-liquid interface waves can be described by:

$c = \sqrt{gh}$ for h/λ< 0.05

$c = \frac{g}{2\pi f}$ for h/λ> 0.5

with

h	Water depth [m]
λ	Wave length [m]

The wave length is related to the wave speed (c) and frequency (f) via:

$$\lambda = \frac{c}{f}$$

An important remark is that in (most) gas-solid systems the effective speed of sound is the gas speed of sound. In liquid-solid systems this is not the case. In a liquid-filled pipe the acoustic speed of sound is a combination of the fluid speed of sound and the wall flexibility:

$$c_a = \sqrt{\frac{E}{\rho_{fluid}}}\left[1 + \frac{D}{d_s}\frac{E}{E_s}\right]^{-\frac{1}{2}}$$

with

E	Fluid bulk modulus [Pa]
E_s	Solid elasticity modulus [Pa]
D	Duct diameter [m]
d_s	Wall thickness [m]

For gas – liquid mixtures, the effective speed of sound is dependent on the distribution (flow regime) of the mixture. For homogenous flow (fully mixed) the effective speed is:

$$\frac{1}{\rho_m c_m^2} = \frac{\alpha_l}{\rho_l c_l^2} + \frac{(1-\alpha_l)}{\rho_g c_g^2}$$

with

c_m	Mixture speed of sound [m/s]
ρ_g	Gas density [kg/m3]
ρ_l	Liquid density [kg/m3]
ρ_m	Mixture density $\rho_m = \alpha_l\rho_l + (1-\alpha_g)\rho_g)$ [kg/m3]
α_l	The liquid hold-up. For fully mixture flow with no slip, this is the volume fraction of liquid (Qliq/(Qliq+Qgas))

In case of more stratified flow (air flow on top of a water film) rather than mixed flow, the effective speed of sound is the air speed of sound.

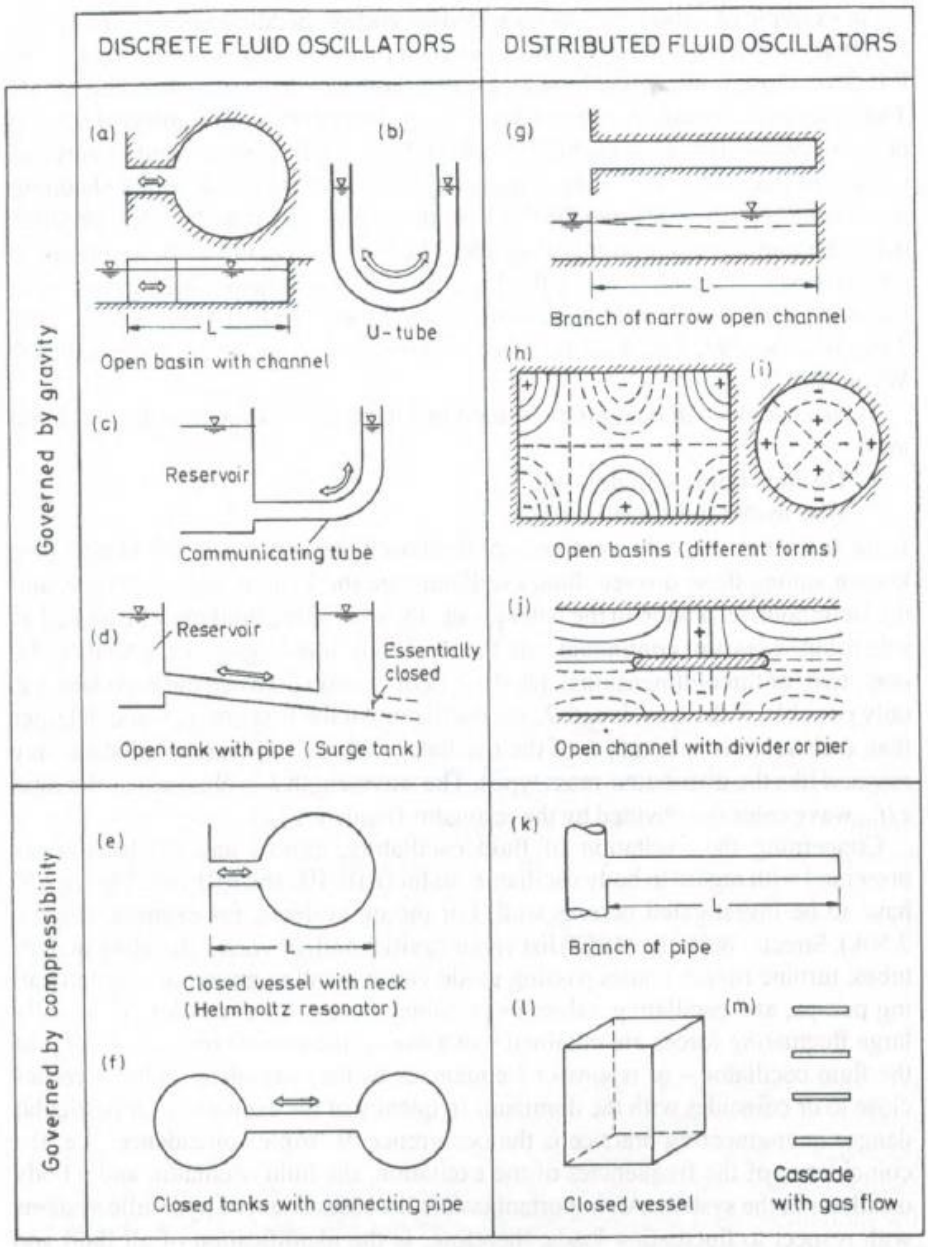

Figure 2.50. Partial 'checklist' for basic fluid oscillators which may give rise to resonance-related fluctuating forces. (Lines in sketches h and j: contours of constant surface-displacement amplitudes for a particular mode).

Figure 23: Overview of main fluid resonators (Nau p70).

The main types of resonances are :

Helmholtz (figure e in Figure 23)

$$f_r = \frac{c_a}{2\,\pi}\sqrt{\frac{A}{l_{eff}V}}$$

c_a Speed of sound in the fluid [m/s]
A Cross sectional area [m2]
V Volume [m3]
l_{eff} Effective length. $l_{eff} = L_{neck} + 2*l'$. l' is the added length to account for 'jets' at the neck lengths. The added length is l'≈ 0.3-0.42*d (with d the neck diameter).

Side branch (closed at one end) (figure k in Figure 23)
The one sided closed sidebranch is one of the classic acoustic resonators. At the closed end, the fluid velocity is always zero and at the open end the pressure (disturbance) is zero. This results in a resonance of

$\lambda_r = \frac{c}{f_r} = \frac{4L_{eff}}{2N-1}$, N = 1, 2, 3, etc
with
L_{eff} Effective length : $L_{eff} = L\left(1 + 0.48\frac{d}{L}\right)^{0.5}$

Open basin (figure h in Figure 23)
The interface instability in a closed (narrow) basin is comparable to a closed-closed pipe system. In both systems the walls acts as full reflection. The main difference is that the wave speed is given by the surface waves and therefore the water depth rather than the fluid compressibility is the important parameter.

For a closed-closed system the resonance frequencies are given by:

$\lambda_r = \frac{c}{f_r} = \frac{2L_{eff}}{N}$, N = 1, 2, 3, etc

This effect of course applies to all directions on the basin.

Utube (figure b in Figure 23)
For a Utube the resonance is given by:

$$f_r = \frac{1}{2\pi}\left[\frac{2g}{l}\right]^{\frac{1}{2}}$$

With
l Length of total liquid column (from surface to surface) [m]

Closed in gas volumes
A special case of a resonance is a closed-in gas volume. This air-pocket can effectively act as a spring.

This for instance occurs at an overspill of water where an air-pocket gets trapped by the liquid. The excitation is in that case the fluctuating (falling) water jet. The typical frequency is in that case given by:

$$f\ T_v = (n + \tfrac{1}{4})$$

with T_v the falling time of the water. Kolkman & Jongeling (K&J A p 109) and Naudascher (Nau p142) describe this mechanism in detail.

For a closed in gas bubble (Figure 24), the effective spring constant of the gas volume is related to the compressibility of the gas

$$k = \gamma A \frac{p}{z}$$

with γ the isentropic coefficient (for air γ=1.4), *A* the surface if the volume [m^2], *p* the pressure [Pa] and *z* the compressibility (for air at atmospheric condition z = 1). If we consider the liquid column as a single mass, the eigenfrequency is given by:

$$f = \frac{1}{2\pi}\sqrt{\frac{g\gamma p}{\rho_l H z}}$$

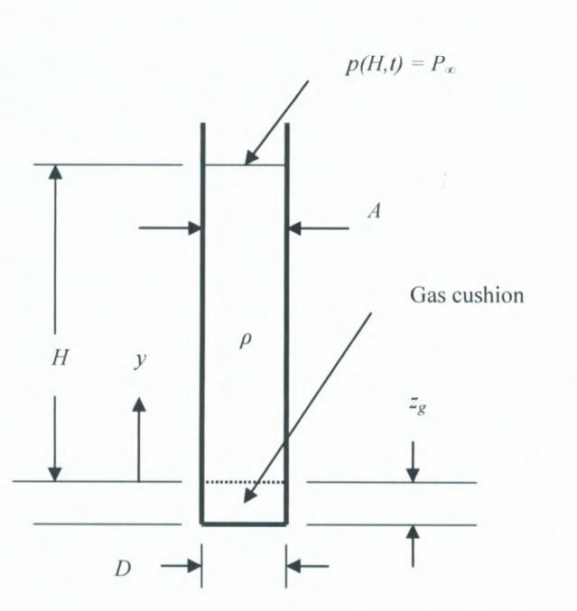

Figure 24: Trapped gas cushion ((Moody, 2007)

4.4.3 *Calculate vortex shedding frequencies behind the gate (horizontal excitation)*

Behind a vertical gate a large recirculation area exists, which results in horizontal forces on the gate. The Strouhal number for this excitation can be found from Figure 25.

The velocity v1 is the velocity below the gate (therefore based on the height δ) without considering any contraction effects [Abelev].

$$v_1 = \frac{Q}{\delta L}$$

with Q the water flux [m^3/s], δ the height beneath the gate [m] and L the width of the gate (perpendicular to the flow)]m.

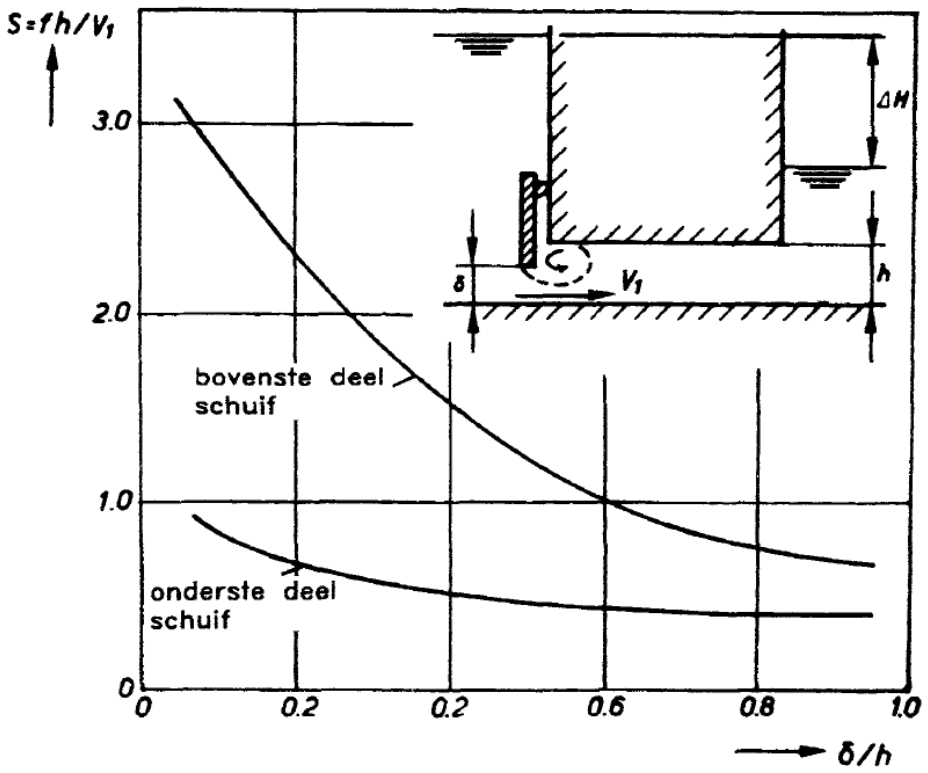

Figure 25: Strouhal number as function of relative gate height (K&J A p85, original Abelev, 1959).

In addition to this graph, Naudascher (N&R) gives an estimation for the horizontal vibrations of gates with underflow (N&R section 9.2.3). Naudascher argues that the horizontal excitation and vertical one are closely linked and also due to vortices traveling below the gate resulting in a non-uniform distribution.

He defines a critical reduced velocity as

$$V_{r,critical} = \frac{V}{fe} \cong \frac{4}{2n-1}, n = 1,2,..$$

In this

e	Gate width (width of section of gate along which vortex travels) [m]
V	Velocity below the gate [m/s]
f	Mechanical natural frequency [Hz]

To avoid this mode, a safety margin should be applied (typically 30%). He further argues that the first two modes (n=1, n=2) are dominant and that the n=3 mode and higher already occur less often (as the amplitude reduces with the mode number). This would lead for the lowest velocity:

$$V_{crit} = 0.7 \cdot f \cdot e \cdot \frac{4}{2 \cdot 2 - 1} = 0.9 \cdot f \cdot e$$

4.4.4 Calculate vortex shedding frequencies below the gate (vertical excitation)

Kolkman & Jongeling prescribe the Strouhal number according Figure 26.

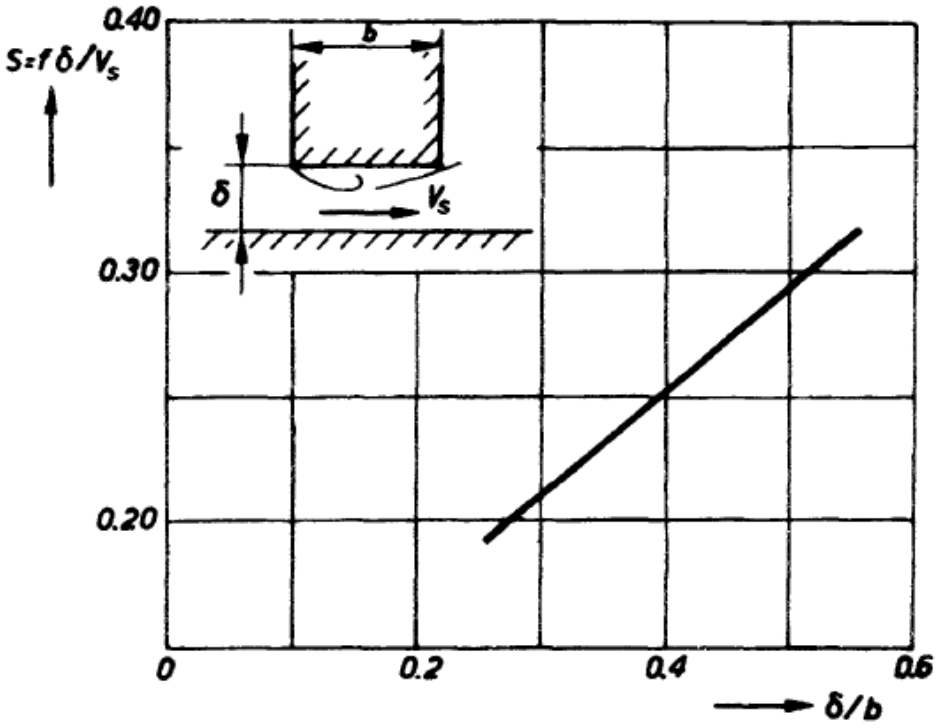

In Figuur A4.2 wordt het dominante Strouhalgetal gegeven voor verticale excitatie aan de onderkant van een schuif.

Figure 26: Strouhal number below a gate (K&J A p86).

In this figure the frequency (Sr = f δ/V_s) is defined based on the gate height as function of relative gate height (δ/b). In this is b in principle the length scale on which the disturbance (vortex) travels before it reached the edge (Figure 27). This means that of the gate is edged only the length on which the disturbance travels.

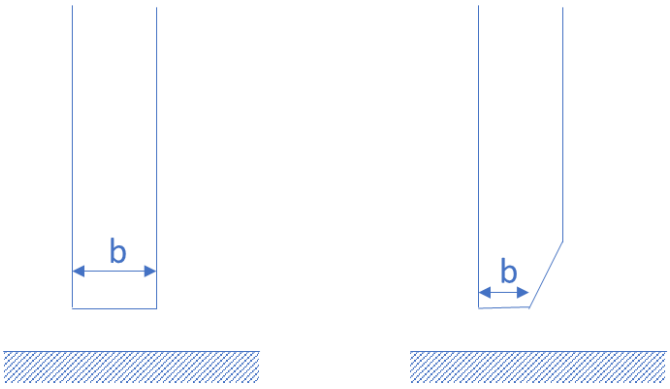

Figure 27: Definition of b.

It must be noted that small geometrical details can change the exact Strouhal characteristic and therefore the Figure 26 is indicative and not universal.

Naudascher prescribes (Nau p344):

$$Sr = \frac{fe}{V} = (n + \varepsilon)\frac{V_c}{V}$$

The parameters ε and V_c/V are very configuration dependent. e is the distance between the leading and impinging edges. For a system with a downstream lip the typical Strouhal number ranges from 0.35 (mode 1) and 0.85 (mode 2) .

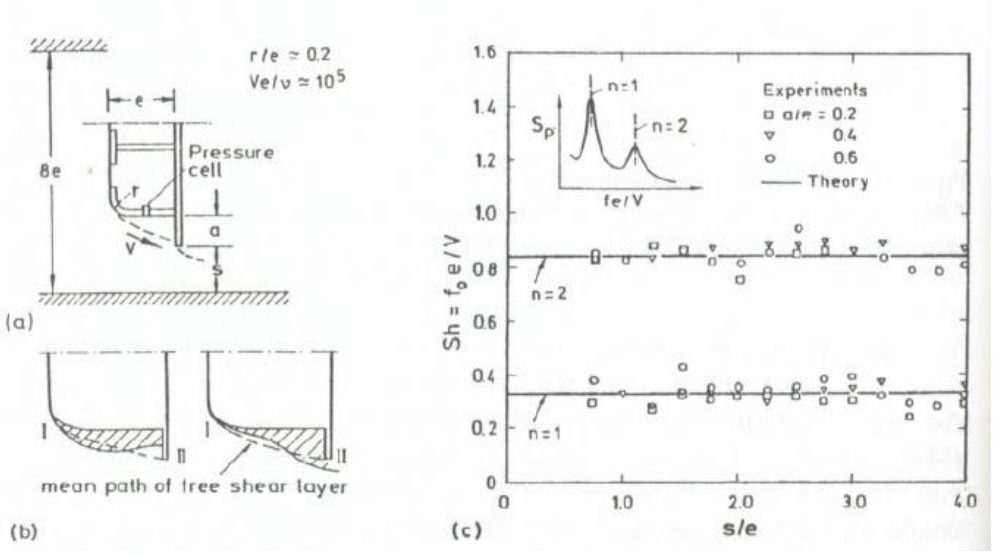

Figure 28: Strouhal number for a gate with an extended lip. (Nau p 138).

He translates this in recommendations of a critical reduced rate for different designs (Figure 29). The reduced velocity is defined via:

$$V_r = \frac{V}{f_n e}$$

with

V Flow velocity below the gate [m/s]
f_n Mechanical natural frequency [Hz]
e gate thickness [m]

For the lowest mode, the critical reduced velocity is : $V_r = 2$. More detailed values are given in Figure 29.

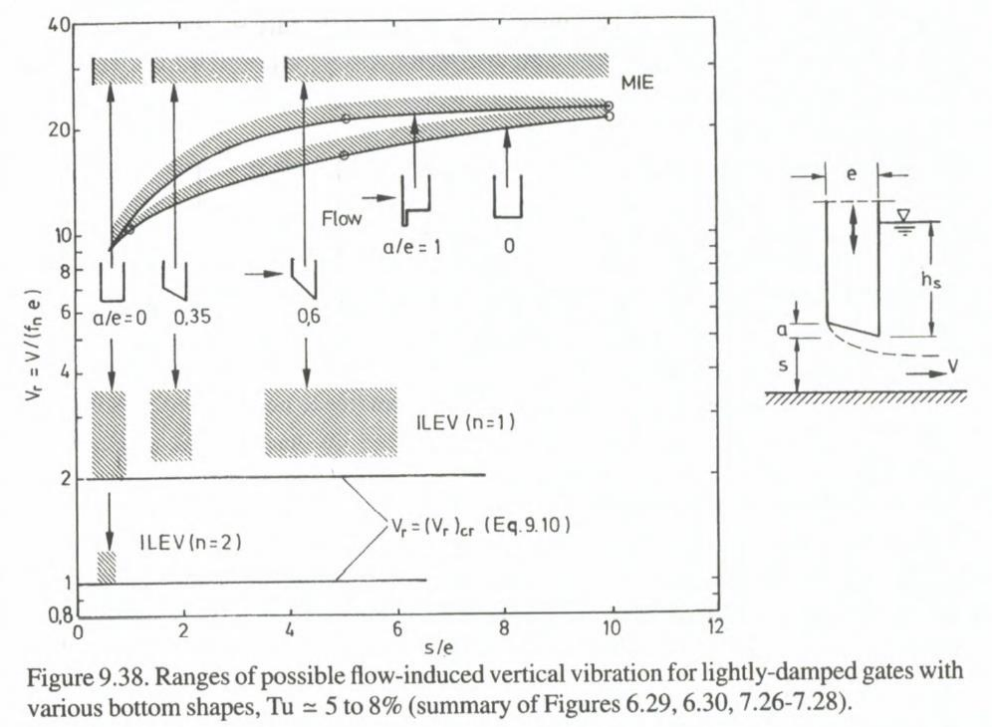

Figure 9.38. Ranges of possible flow-induced vertical vibration for lightly-damped gates with various bottom shapes, Tu ≃ 5 to 8% (summary of Figures 6.29, 6.30, 7.26-7.28).

Figure 29:Critical reduced velocity for vertical excitation (Nau p 349). MIE is motion induced excitation. ILEV stands for impinging leading-edge vortices.

Overall the range of Strouhal number for the dominant mode 1 is between Sr = 0.2 – 0.4. Either this Strouhal range or the results from Figure 29 must be used for evaluation.

4.4.5 Calculate vortex shedding frequencies at/for gate elements

Any bluff body can be subjected to dynamic drag and lift forces due to vortex shedding. The figures are given in Annex D. The figures included are:

Strouhal number for

- Cylinder (K&J A124), (Kaneko p15)
- Cylinder in a channel (K&J A155)
- Bluff bodies with rounded edges (K&J A131), (Kaneko p72, 73, 74),(Blevins p50)
- General bluff bodies (K&J A p152), (Blevins)
- Straight edged beams (K&J A p126)
- Plate structures with different length/thickness ratio (K&J A p157), (Kaneko p74)
- Plate structures with different inclination angle (K&J A p157), (Blevins p51)

4.4.6 Compare mechanical, resonance and excitation frequencies.

In Section 4.3 a discussion is given in typical safety margin. For avoiding all vibrations (including in the drag direction) a margin of 0.35 is recommended. This is build up out of a factor half for the general frequency in the drag direction and a safety margin of 0.7).

4.4.7 Evaluate galloping mechanism

To evaluate any potential for galloping the effective damping must be evaluated. The base criterion for galloping is (Den Hartog)

$$\frac{dC_L}{d\alpha} + C_D < 0$$

With C_L the lift and C_D the drag coefficient and α the angle of attack. This means a critical parameter is dependent on the lift coefficient as function of the inclination angle. The drag and lift coefficient can be obtained assuming quasi steady state if V/(f·h) > 10). In this V is the upstream velocity, f the natural frequency and h the body dimension. A number of graphs are available for different shapes which give this parameter.

The critical velocity is in that case given by [Blevins p108]:

$$\frac{V}{fD} = \frac{4m\xi\omega}{\rho D^2} \Big/ \frac{\partial C_y}{\partial \alpha}$$

With m the total mass (including added mass effects), D the typical dimension of the body [m], ξ the mechanical damping factor [-].

Several handbooks provide overviews of the lift coefficient as function of angle for a number of shapes. For example:

- K&J A p142
- N&R p209
- Kaneko P77

These figures are reproduced in Annex E

In general this analysis is given for bodies fully immersed (bluff bodies, cables etc). Nguyen & Naudascher used a similar analysis for gates. They found that the criterion for stability for galloping can be replaced by the slope of C_L vs s/e (s gate height and e gate thickness) [N&R p 208-209]. A positive slope indicates a danger of soft excitation due to galloping, unless either Sc is larger than a critical value or the maximum V_r is smaller than $V_{r,crit}$.

Chapter 3.3 in Naudasher gives Cl (or κ) as function of s/e for different shapes. This gives a clear indication of which shapes are susceptible or not for galloping. The main figures are given in Annex E.

4.4.8 Evaluate potential changing discharge coefficient

The discharge coefficient changes with changes in the gate position. This can result in a non-linear feedback between the position of the gate and the flow through the gate.

4.4.9 Evaluate potential changing non-constant separation points

If the edge is very rounded and the flow pattern is expected to change significantly with a change in valve position, the potential of a non-constant separation point might occur (Figure 30). The separation point of the flow on a rounded body is dependent on the flow velocity. If the total pressure drop across the gate is

dependent on the separation point this can result in a time-dependent separation point. This in general occurs at lower velocities.

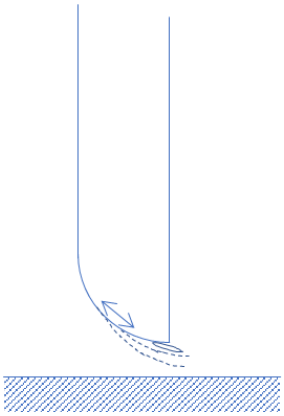

Figure 30: Change in separation point (dashed lines gives potential separation points).

4.4.10 Evaluate momentum upstream & downstream of valve ('bath plug' mechanism)

Naudasher gives the following statements:

- Devices controlling flow through small openings are susceptible to movement-induced excitation if they are press-shut devices and exposed to large fluid-inertia effects from adjacent flow passage (N&R p 233, Figure 31)

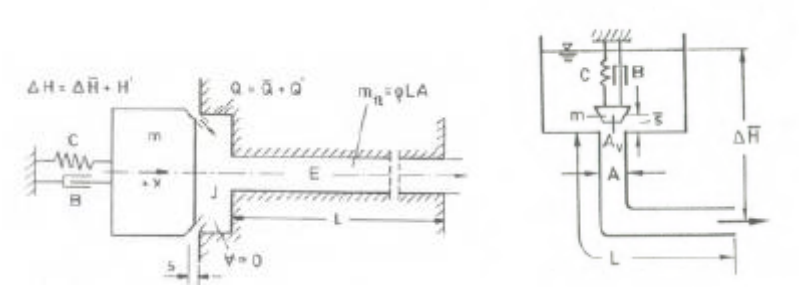

Figure 31: Examples of press-shut devices (Figure 7.45 Nau p 231, Figure 7.46 Nau p 232).

- Valves controlling the outflow from a Helmholtz resonator of negligible fluid inertia are susceptible to movement-induced excitation if they act as press-open devices (N&R p230, Figure 32)

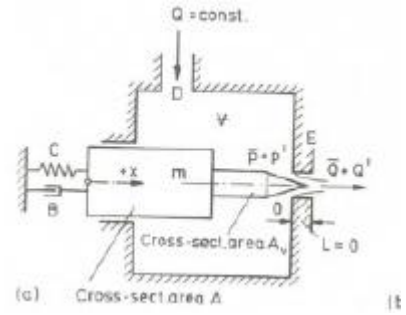

Figure 32: Example of press-open device (Figure 7.44 Nau p 229).

Typical examples of these statements are given in Figure 33 (e) and (j). The general statement to be made in this is:

“When the fluid-inertia forces accompanying the discharge variations are such that they act in the direction of body-speed, energy will be transferred to the body and Motion-Induced-Excitation will be complete” [Nau p 60].

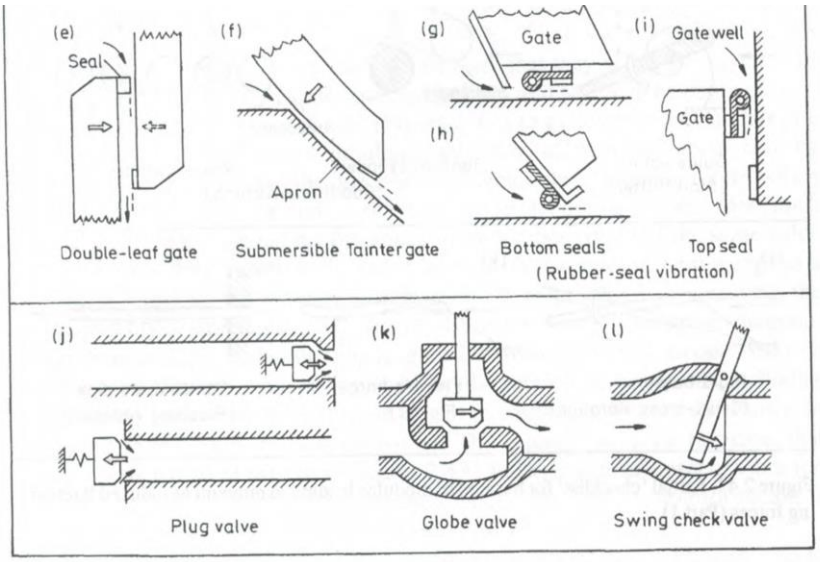

Figure 2.44. Partial ‘checklist’ for basic MIE modules leading to movement-induced fluctuating forces (Part 2).

Figure 33: Examples of inertia important feedback (Nau p62).

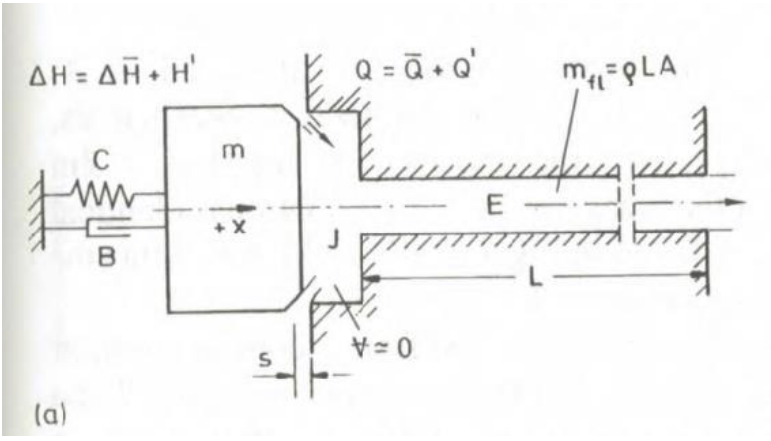

Figure 34: Definitions for stability criterion.

For such a system the stability criterion can be written as (N&R p 231):

$$\frac{2\gamma\Delta\bar{H}}{C/\sqrt{A_v}} \leq \frac{\bar{s}}{\sqrt{A_v}}$$

with

ΔH	Hydrostatic head across the valve
γ	Specific weight of fluid (ρg)
C	Spring stiffness
A_v	Effective cross-sectional area of valve plug
s	gap width [m]

Important in this is that the fluid body acts as inertia ($L << c_a T/4$) with L the length of the pipe, c_a the speed of sound and T the period (1/frequency).

As stated in the theoretical part, this criterion assumes linear perturbations. If the valve is hitting the seat, the fluctuations will become large and highly non-linear.

4.5 Screening summary

As a repeat from section 4.2, the steps are repeated but now with references to the individual graphs required for screening. The screening steps are :

1. Calculate mechanical eigen frequencies
2. Check horizontal excitation (Figure 25, criterion Naudascher)
3. Check vertical excitation (Figure 26)
4. Check for any large structures which are fully submerged and calculate Strouhal number for vortex shedding on these elements
5. Check for large enclosed cavities for vortex shedding in cavities
6. Calculate upstream and downstream acoustic resonances (calculate first modes for channel in which valve/gate is situated, calculate resonance frequency for channels/pipes in which valves are situated) (section 2 in this chapter)
7. Check for designs for low susceptibility for galloping (see designs Nau section 3.3)
8. Check for potential for MIE (‘bath plug’): Is there an adjoining water mass for which the inertia works ‘the wrong way’

5 Examples

5.1 Discussion – case 1

An example of a seal system is given in Figure 35 with a detail of the seal construction in Figure 36.

The original discussion is on why the ‘right’ (“Maar zo”) option is better than the left (“Niet zo”) option. Arguments given were:

- Adding the lip reduced the effective ‘force’ area
- Adding the lip results in a more fixed separation point where vortex shedding is more fixed
- Adding the lip adds a more fixed pressure drop across the bottom seal and therefore will be less susceptible to changes in position.

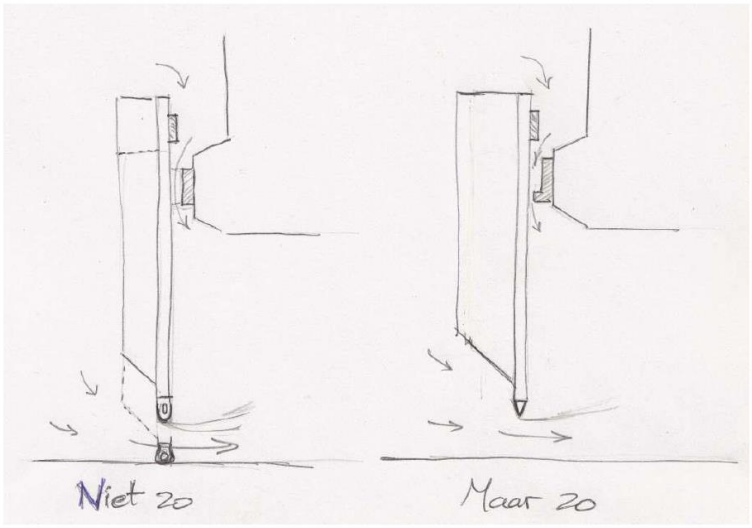

Figuur 1: Rioolschuif

Figure 35: Example as provided by RWS.

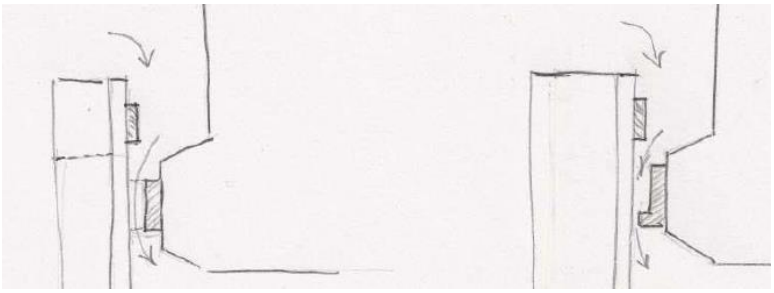

Figure 36: Detail of example as provided by RWS.

If one would turn the figure, the ‘wrong’ configuration looks like a vertical gate in which the a number of mechanism play a role:

- Vortex shedding beneath the gate
- Changes in flow rate with a change in position as a movement up or down will result in a change in flow profile to the gate due to the top seal

In the ‘correct’ design the vortex shedding is mainly on the tip and is more fixed. Furthermore, the pressure drop is more fixed at the bottom seal further limiting the change in flow rate due to movement.

A similar problem is discussed by Kolkman (Kolkman, Development of vibrating-free gate design: learning from experience and theory, 1980) (Figure 37). The example is not completely the same as the top seal is larger than the bottom one. One of the solution suggested was to change the bottom and top seal.

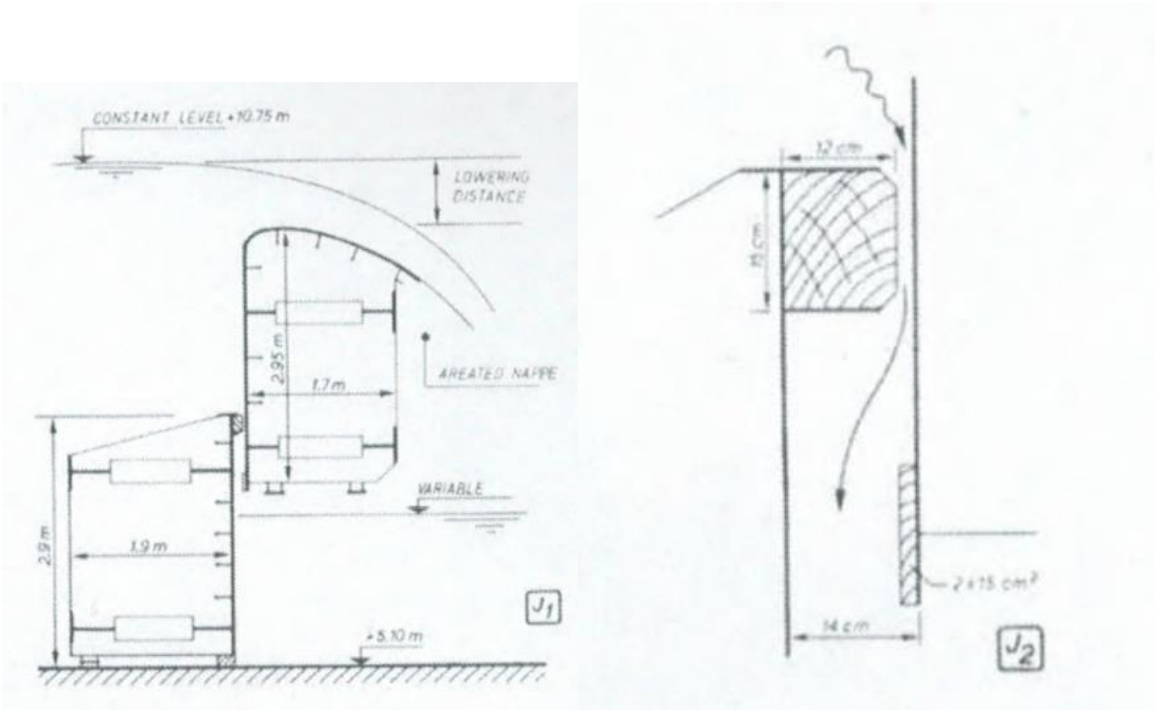

Figure 37: Sketches (Kolkman, Development of vibrating-free gate design: learning from experience and theory, 1980)

6 General statements

In this section some general useful remarks made by the different authors of the reference books are gathered.

- ILEV (impinging leading-edge vortices) induced excitation of gate plates are limited to a narrow range of gate openings (s< 2e) [N&R p 357]
- Only lightweight, lightly damped, flexible structures such as signs, chimneys, towers, suspensions bridges and ice-coated power lines gallop [Blevins p 110]
- Movement induced excitation of vertical gate vibration is a mixture of (1) galloping and (b) excitation involving inertia coupling with fluid-flow pulsations [N&R p 210]
- The regions of transition from flow that is always attached to the trailing edge of the gate lip to the completely separated flow are represented in figure 3.24. Since this transition is unstable and leads to pressure fluctuations which might excite gate vibration, it is advisable to choose a lip shape with e*/d well above the critical values given in Figures 3.24 [Nau p 154].
- Shapes sensitive to vertical and horizontal vibrations:

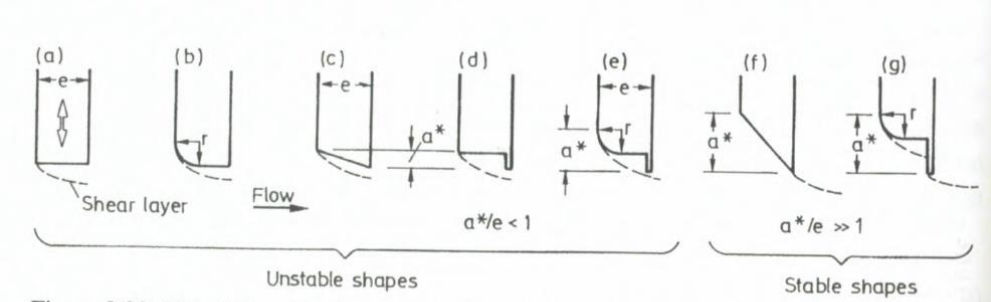

Figure 9.39. Unstable and stable bottom shapes for gates free to undergo vertical vibrations (qualifications given in text).

Figure 38: (N&R p350)

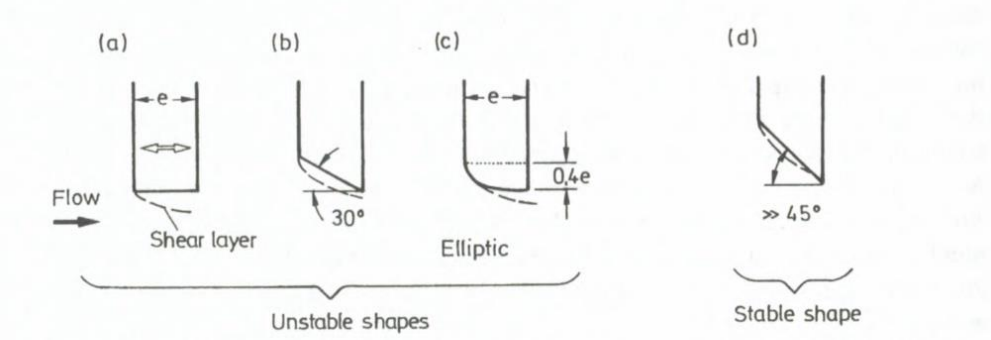

Figure 9.46. Unstable and stable bottom shapes for gates free to undergo horizontal vibrations.

Figure 39: (N&R p 356)

- Regarding motion induced excitation: “When the fluid-inertia forces accompanying the discharge variations are such that they act in the direction of body speed, energy will be transferred to the body and MIE will be complete” (Nau p 60)
- For gates, the excitation due to (upstream) turbulence plays a minor role as the resonance frequency is in general higher than the main fluid frequencies and because the fluid frequency spectrum is a broadband excitation [K&J A p18]
- There are no known examples where a resonance of the basin-pipe system lead to problems [K&J A p51]
- For pumps and turbines: If dH/dQ>0, the system can become unstable
- Critical gap widths are for opening 2-3 times the plate thickness. If the gate is rounded this range increases [K&J A p 226]

7 Discussion and recommendations

In this report, the currently used screening methods for flow-induced vibrations on gates and valves are discussed.

In addition to the current rules the following screening has been extended:

- Screening for horizontal vibrations on gates. This might be especially important for newer lighter structures.
- Additional evaluation methods for vertical vibration.
- Additional evaluation for galloping in underflow gates.

The most uncertain evaluation remains motion-induced self-excitation in which the upstream/downstream liquid inertia plays an important role.

The following recommendations are made:

- Put the current design guidelines as used by RWS (and as discussed in this document) next to the recommendations as for instance given in “U.S. Army Corps of Engineers, 2014, “DESIGN OF HYDRAULIC STEEL STRUCTURES””. The detailed recommendations given for seals and detailed gate design might be very beneficial.
- Perform CFD simulations on a gate valve with 60 degree baffle. This is the currently proposed base design for gates. Therefore, a dedicated screening figure with respect to forcing characteristic and Strouhal number are required.
- Perform CFD simulation to evaluate the potential of self-excitation based on steady state simulations. The input from CFD including estimations of the upstream and downstream momentum might lead to a more accurate indication of vibrations.

8 Bibliography

Abelev, A. (1959). Investigations of the total pulsating hydrodynamic load acting on bottom outlet sliding gates and its scale modelling. 8th congress. Montreal: International association for hydraulic research.

Billeter, P., & Staubli, T. (2000). Flow-Induced multipple-mode vibrations of gates with submerged discharge. Journal of FLuids and Structures.

Blevins, R. (2001). Flow-Induced Virbations. second edition. Malabar: Krieger Publishing Company.

Engineers, U. A. (2014). Design of Hydraulic Steel structures. US Army Corps of Engineers.

Erbisti, P. (2014). Design of Hydraulic Gates - 2nd edition. London: Taylor & Francis Group.

Erdbrink, C. (2013). Controlling flow-induced vibrations of flood barrier gates with data-driven and finite-element modelling. In Comprehensive flood risk management.

Erdbrink, C. (2014). Modelling flow-induced vibrations of gates in hydraulic structures. PhD thesis TU Delft.

Kaneko, S., Nakamura, T., Inada, F., & Kato, M. (2008). Flow-Induced Vibrations. Classifications and lessons from practial experiences. Oxford: Elsevier.

Kolkman, P. (1976). Flow-induced gate vibrations. . PhD thesis TU Delft.

Kolkman, P. (1980). Development of vibrating-free gate design: learning from experience and theory. Practical eperiencnes with flow-induced vibrations. Springer.

Kolkman, P., & Jongeling, T. (1996). Dynamisch gedrag van waterbouwkundige constructures (deel A, B en C). Rijkswaterstaat, Dienst Weg- en Waterbouwkunde.

Moody, F. (2007). Acoustic amplitifcation of a vertical liquid column bouncing on a gas volume. ASME-PVP. San Antonio: ASME.

Nasser, M. (n.d.). Flow-induced vibrations and galloping gates.

Naudasher, E. (1991). Hydrodynamic forces. Rotterdam: A,A, Balkema.

Naudasher, E., & Rockwell, D. (1994). Flow-Induced Vibrations. New York: Dover Publications.

Naudasher, E., Kobus, H., & Rao, R. (1964). Hydrodynamic analysis for high-head leaf gates. Journal of the Hydraulics divisions.

Paidoussis, M., Price, S., & De langre, E. (2013). Fluid-Structure interactions. Cross-flow-induced instabilities. Cambridge University Press.

Testud, P., Aurgean, Y., Moussou, P., & Hirschberg, A. (2009). The whistling potentiality of an orifice in a confined flow using an energetic criterion. Journal of Sound and Vibration, 769-780.

Thang, N., & Naudascher, E. (1986). Self-excited vibrations of vertical-lift gates. Journal of hydraulic research.

Thang, N., & Naudascher, E. (1986). Vortex-induced vibrations of underflow gates. Journal of Hydraulic research.

Violato, D., De Jong, B., & Golliard, J. (2016). Universal scaling for broadband turbulent noise in internal flow devices. FIV 2016. The Hague: TNO.

Weaver, D., & Adubi, F. K. (1978). Flow induced vibrations of a hydraulic valve and their elimination. Journal of Fluids Engineering.

Weaver, D., & Ziada, S. (1980). A theoretical model for self-excited vibrations in hydraulic gates, valves and seals. Journal of pressure Vessel technology

9 Signature

Delft, October 2017 TNO

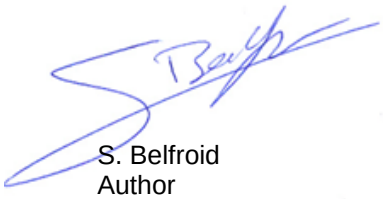

E.D. Nennie
Research Manager
Heat Transfer and Fluid Dynamics

S. Belfroid
Author

A Classifications

A.1 Introduction

In this Annex, a number of different classifications are presented. These classifications of course are very similar but they often provide also a structure for screening.

A.2 Kaneko

The classification of Kaneko is mainly aimed at fully immerged structures. That is, there is a complete flow around the object but it also covers internal flow. But it does provide a good overview of the different mechanisms and how fast the classification 'tree' can explode. In this section, only the tree for single phase flow is covered. The basic structure is given in Figure 40. This results in three main subdivisions:

- Turbulent excitation
- Vortex shedding
- Fluid-elastic vibrations (self-excitation such as galloping, flutter)

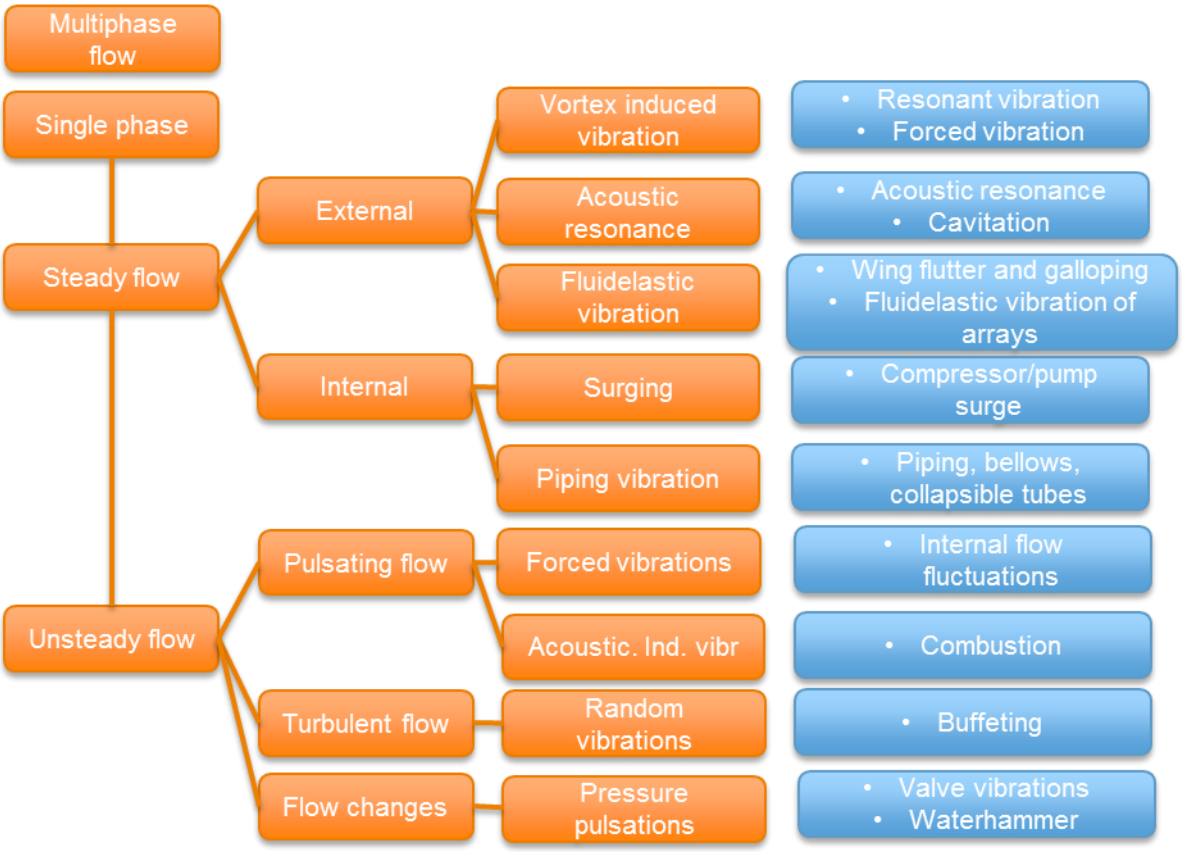

Figure 40: Basic classification structure (Kan p7).

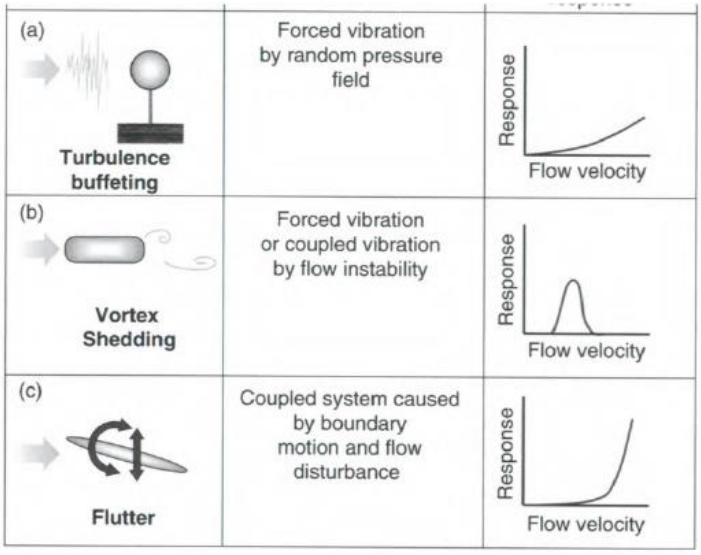

Figure 41: Example of main mechanisms.

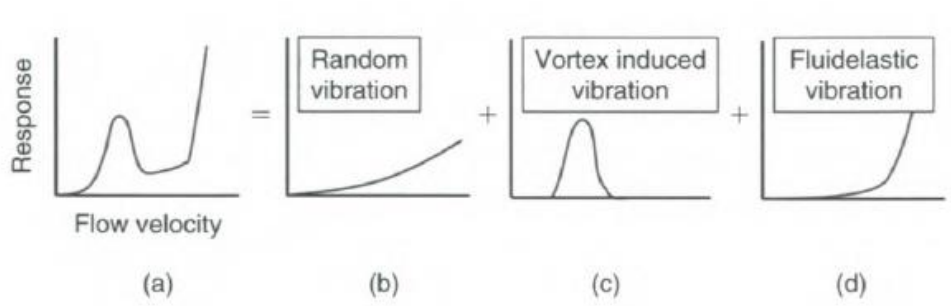

Fig. 1.8 Vibration of tube array caused by cross-flow.

Figure 42: Response of mechanical structure due to different excitation mechanisms.

The classification can be structures as:

- Vibrations induced by cross-flow
- Vibrations induced by extremal axial flow
- Vibrations induced by internal fluid flow
- Vibrations induced by pressure waves in piping

A.3 Naudascher

Naudascher subdives the vibrations and excitation mechanisms in four major groups. In this section these main groups are briefly described.

- Predominantly extraneously induced excitation (EIE) (N&R, Chapter 5; Nau 2.2.1)
    - Earthquakes
    - Machine and machine parts
    - Turbulent buffeting

This concerns excitation due to turbulence generated upstream of the structure.

    - Cavitation and two-phase flow
    - Oscillating flow and waves

This mechanisms are not covered directly. But for instance the turbulent buffeting might sometimes be important. For instance in spillways of very high flow rates with upstream bend or orifice structures. Guidelines and estimation methods for predicting the downstream disturbances are present for pipe systems with single phase flow [Golliard] and to a lesser degree in multiphase flow.

- Predominantly instability induced excitation (IIE) (N&R, Chapter 6; Nau 2.2.2)
    - Vortex shedding

This concerns vortex shedding on bluff bodies and rounded edges.

    - Impinging shear layer

This concerns shear layer impinging on a structure. For instance a shear layer at a cavity or a structure in an jet.

    - Interface instability

This concerns for instance gas trapped below a water spill.

    - Bi-stable instability

This concerns systems in which the flow can be in different stable modes. The system can switch between these modes depending on disturbances.

    - Swirling instability

This concerns flow in for instance a cyclone or flows with three dimensional structures (bends in different planes) in which the swirl in the flow can be stable.

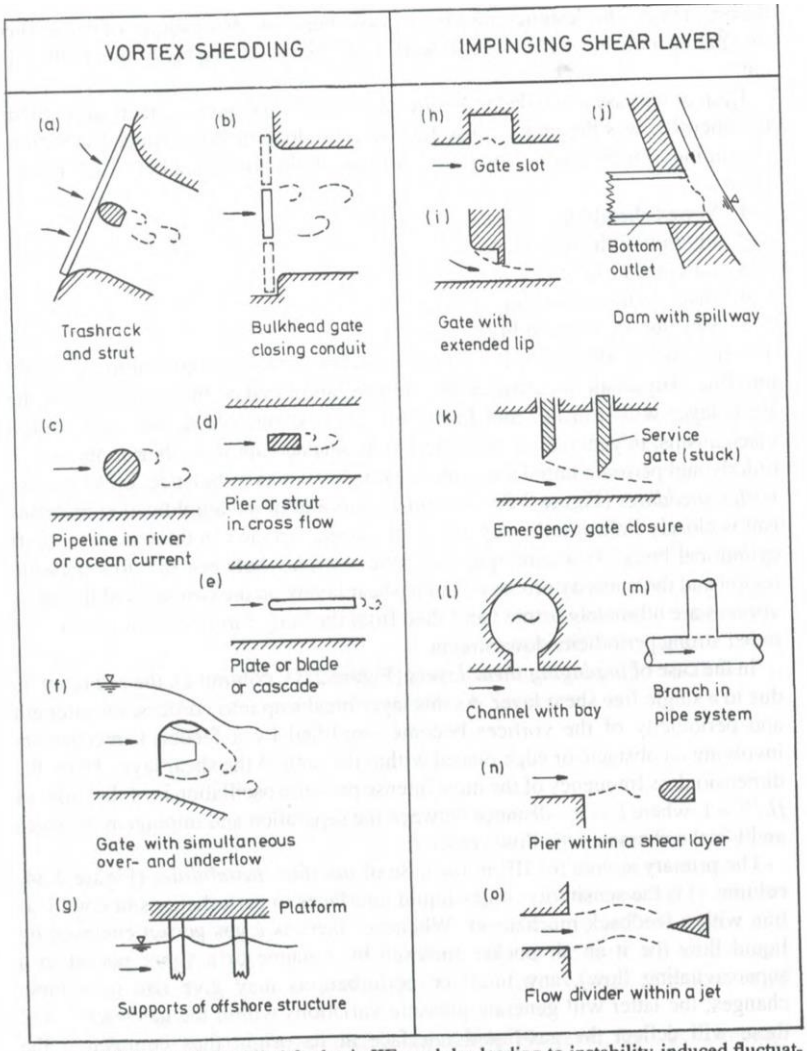

Figure 2.33. Partial 'checklist' for basic IIE modules leading to instability-induced fluctuating forces (Part 1).

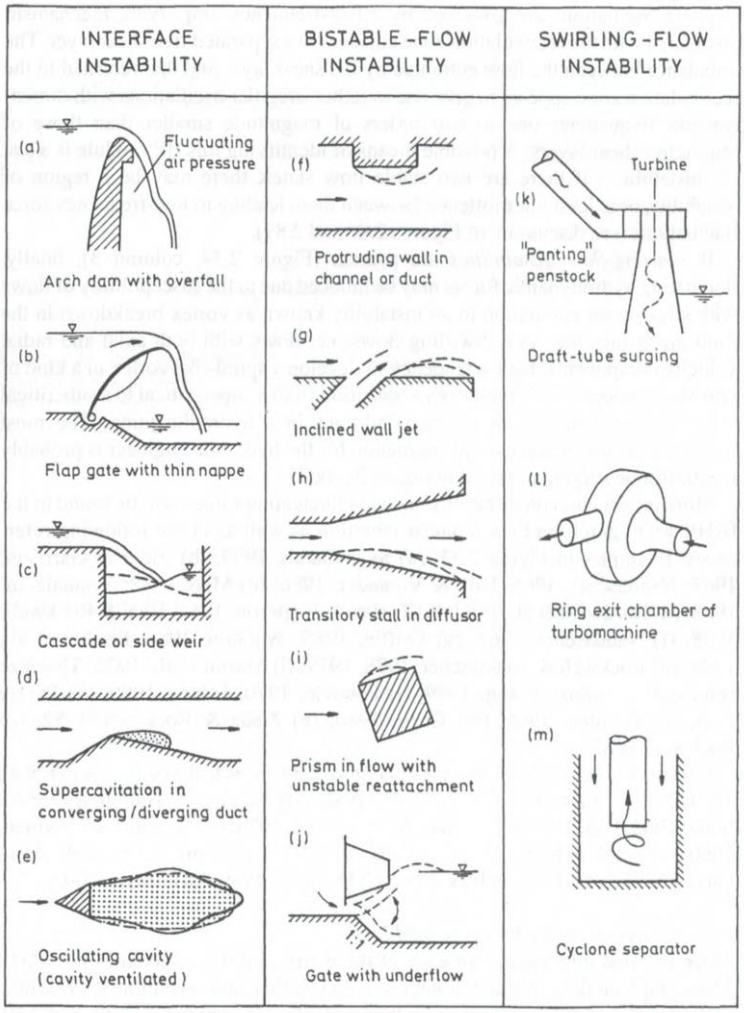

Figure 2.34. Partial 'checklist' for basic IIE modules leading to instability-induced fluctuating forces (Part 2).

- Predominantly movement induced excitation (MIE) (N&R, Chapter 7; Nau 2.2.3)
    - Single mode, negligible coupling

This involves mechanisms such as galloping and (stall) flutter. The mechanical body still has only one degree of freedom.

- Fluid coupling involving discharge variations

In this category there is a pulsating inflow rate or discharge rate

- Mode coupling and multiple body coupling

In this category multiple mechanical modes interact such as in flutter.

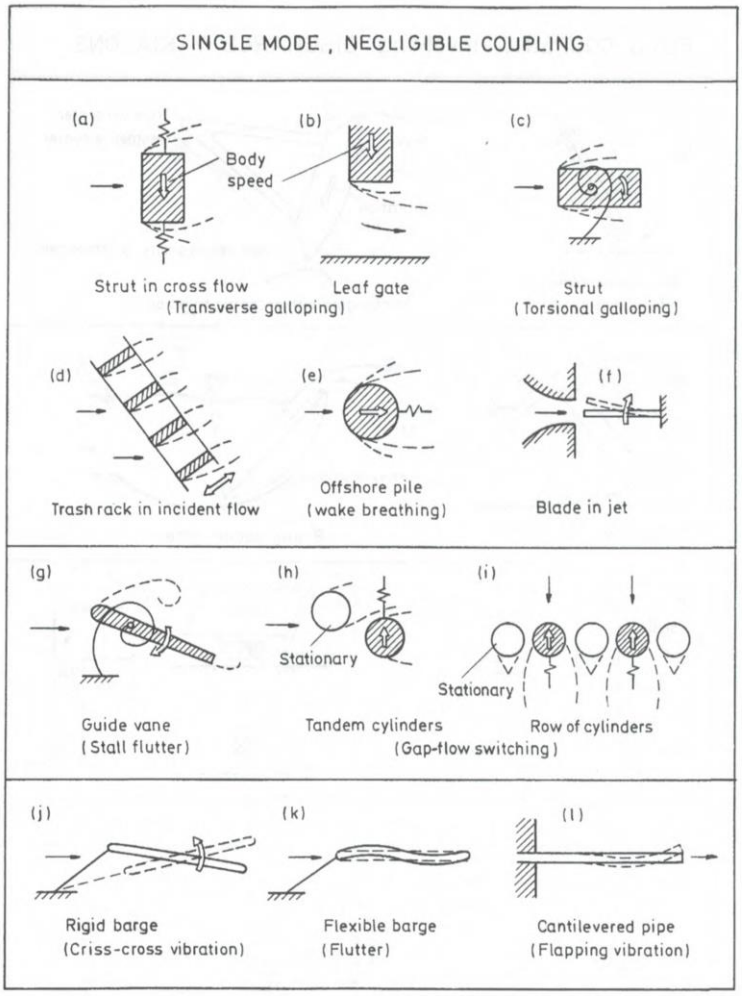

Figure 2.43. Partial 'checklist' for basic MIE modules leading to movement-induced fluctuating forces (Part 1).

Figure 43: Motion induced excitation with single mode, negligible coupling (Nau p 61)

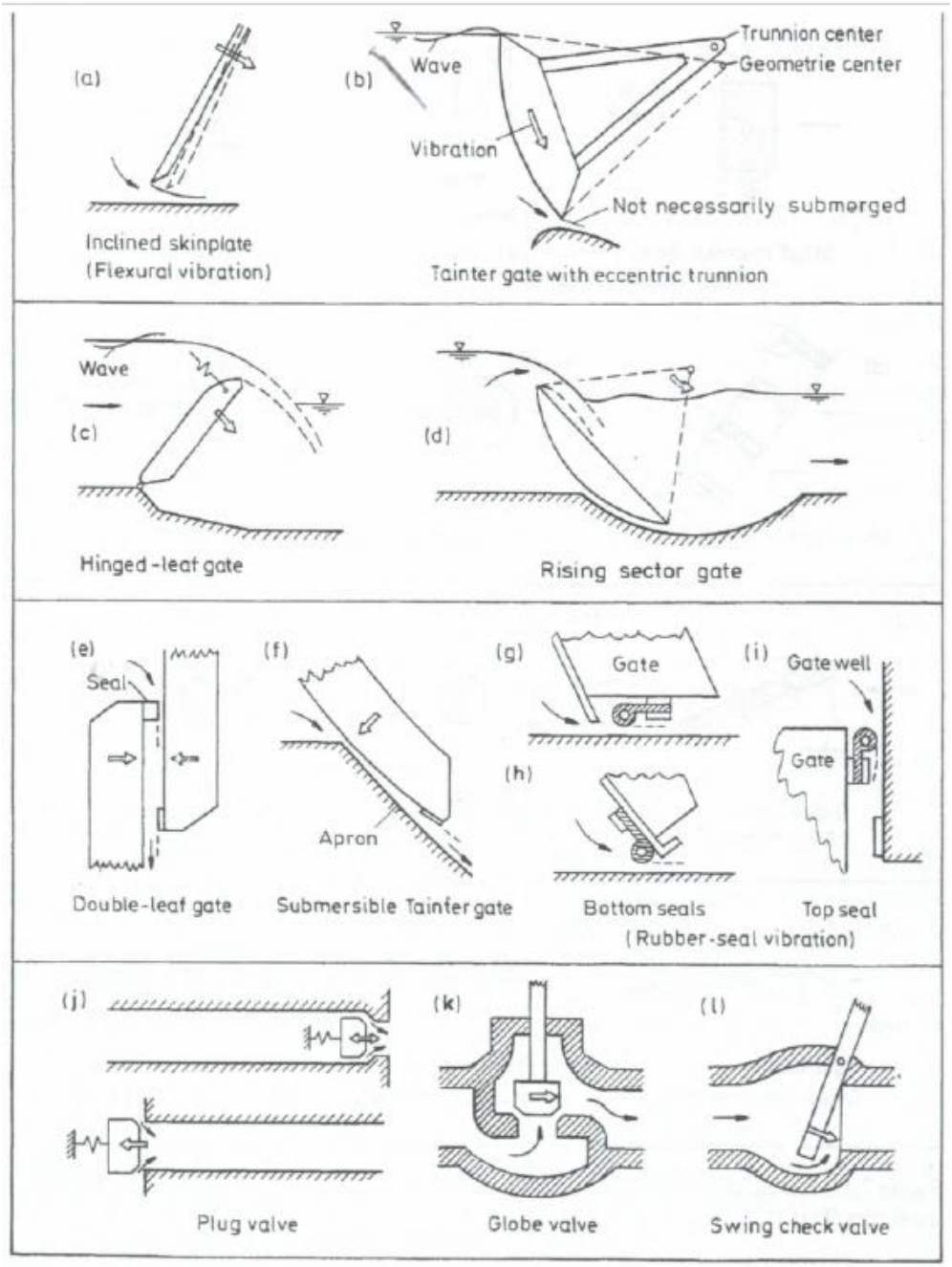

Figure 44: Motion induced excitation with Fluid coupling involving discharge variations (Nau p 62)

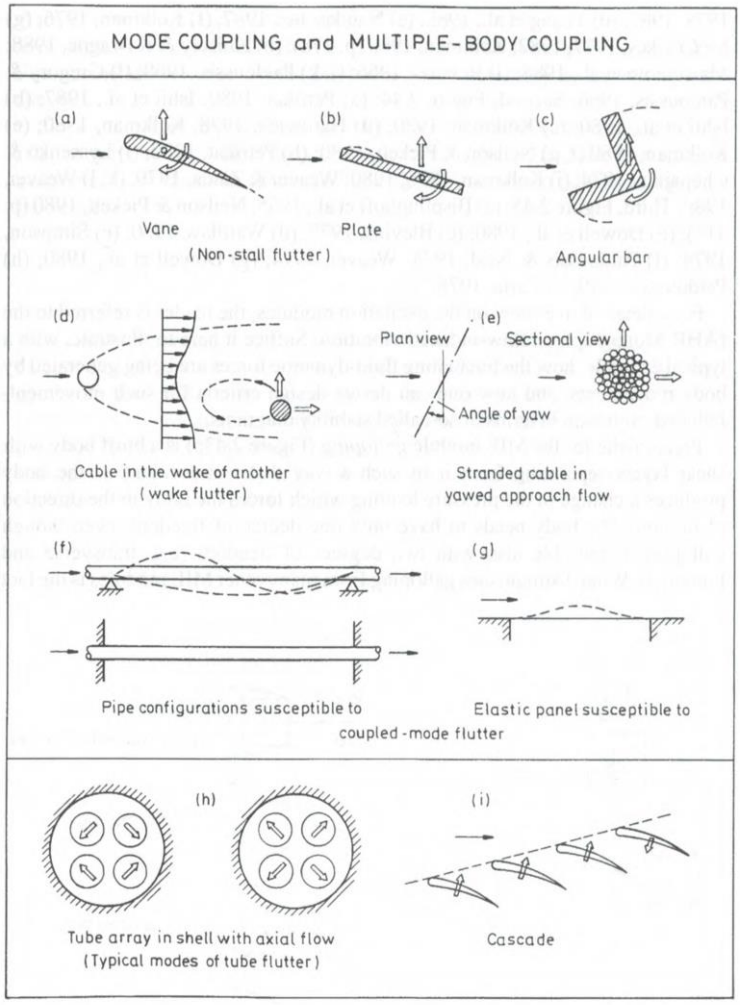

Figure 2.45. Partial 'checklist' for basic MIE modules leading to movement-induced fluctuating forces (Part 3).

Figure 45: Motion induced excitation with mode coupling and multiple-body coupling (Nau p 63).

- Excitation mainly due to a resonator fluid oscillator in a system (N&R, Chapter 4; Nau 2.2.4)
    - Discrete fluid oscillation

This involves resonances such as Helmholtz resonators. This means that the fluid acts as a single mass and the body length is much smaller than the wave length

    - Distributed fluid oscillations

This involves for example resonances in a sidebranch or on the air/water interface. This means that the water body much be seen as a series of masses and that the body length is longer or in the same length as the wave length.

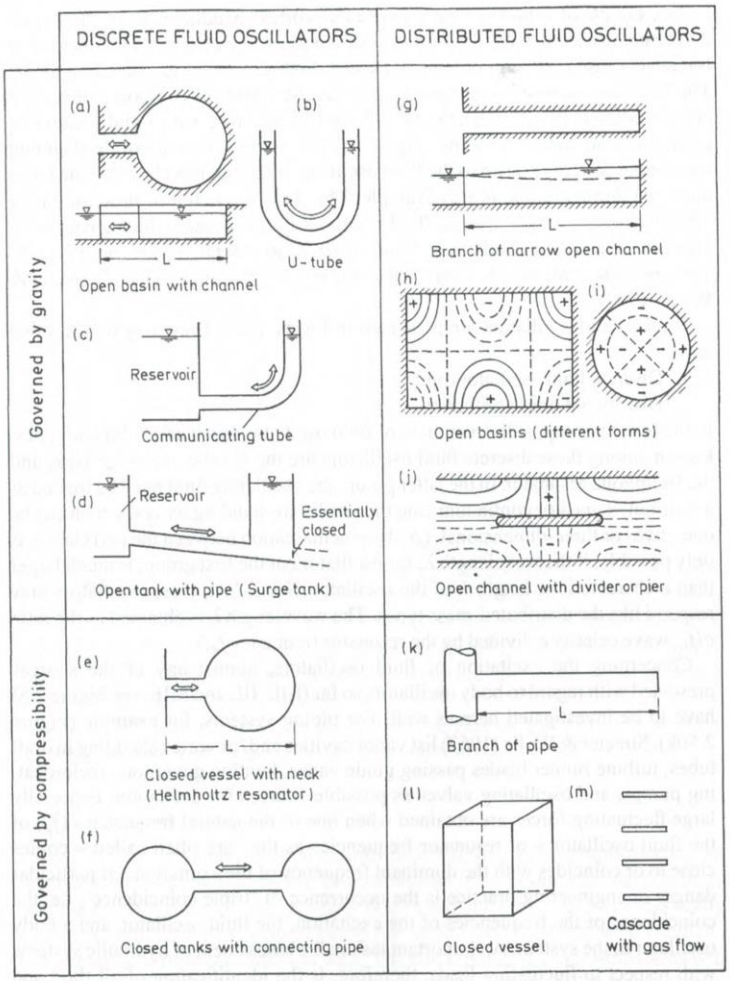

Figure 2.50. Partial 'checklist' for basic fluid oscillators which may give rise to resonance-related fluctuating forces. (Lines in sketches h and j: contours of constant surface-displacement amplitudes for a particular mode).

Figure 46: Fluid oscillators (Nau p 70).

A.4 Kolkman & Jongeling

Kolkman & Jongeling subdivide the excitation/vibration into 5 main excitation mechanisms:

- Turbulence upstream and downstream of object
- Shear layer instabilities (vortex shedding)
- Movement induced excitation
- Enhanced excitation due to fluid resonances
- Fluid resonances due to self excitation

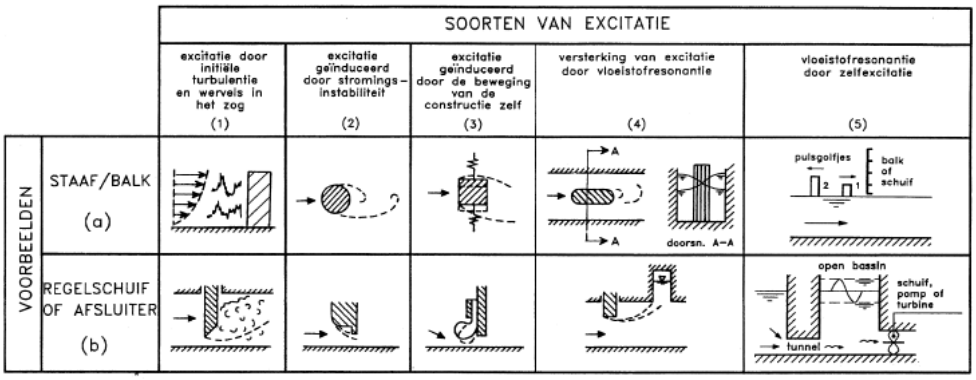

Figure 47L Overview of excitation mechanisms (K&J p 24).

A.5 Erdbrink

The classification according to Erdbrink is very similar to Kolkman & Jongeling. He subdivides the excitation and vibrations in the 5 categories:

- Turbulence
- Stable vortex shedding
- Flow instabilities

This covers:

- Flow separation position is not fixed
- Unstable re-attachment position
- Closed volume due to ‘fixated’ re-attachment position

- Self excitation

This covers:

- Galloping
- Fluctuating leakage gap (‘plug valve’)
- Fluctuating discharge coefficient

- Unstable fluid resonance

B Screening procedures

B.1 Introduction

In this section, different screening procedures are described.

B.2 Standards

In different industries different recommendations, guidelines and standards are used with respect the fluid induced forces.

B.2.1 Nuclear industry

In the nuclear industry guidelines for vortex induced forces for vortex shedding on tubes and tube bundles are present. These described the recommended spacing between mechanical and vortex shedding frequency or the required mechanical damping.

These are:

- ASME Code sec III, Div 1, Appendix N, 1300 series
- JSME S012 (turbulent excitation)

B.2.2 Process engineering

For the process industry guidelines are present to limit the fluid induced forces on piping. These are for instance described in:

- Energy institute, AVIFF

One section covers the vortex shedding on bluff bodies such as erosion probes or thermowells.

B.2.3 Civil engineering

The ASCE and Army corps of engineers are both institutes which publish guidelines and standards for the design of gates. No clear design standards were found for vibrations. Some limited guidelines were found:

- U.S. Army Corps of Engineers, 1997, “Structural Design of Closure Structures for Local Flood Protection Projects”
- U.S. Army Corps of Engineers, 2014, “DESIGN OF HYDRAULIC STEEL STRUCTURES”
  This document gives requirements on the design of seals and details of gate designs.

B.3 Screening procedure Kolkman & Jongeling

K&J describe the following procedure steps in Book C p13:

1. Calculate the mechanical eigenfrequencies and eigenmode shapes.
2. Evaluate turbulent excitation peak frequencies due to recirculation downstream of the construction

3. Evaluate vortex shedding frequencies
4. Evaluate self-excitation (‘bath plug’) mechanism

It must be notes that in this screening no other mechanism of self-excitation are covered and that fluid resonances are not covered.

B.4 Screening procedure Naudascher

Naudscher gives the following recommendation for screening steps:

- Determine body oscillators
- Determine fluid oscillator
- Determine ‘parametric’ excitation (non constant mass, damping, spring coefficients)
- Determine extraneously induced excitation
    - Turbulence, cavitation and two phase flow
    - oscillating flow including waves
    - machine and machine parts
    - earthquackes
- Determine instability induced excitation
    - Vortex shedding
    - Impinging shear layers
    - Interface instability
    - Bi-stable flow instabilities
    - Swirling flow instabilities
- Determine movement induced excitation
    - No coupling
    - Coupling with fluid-flow pulsations
    - Mode coupling
    - Multiple-body coupling

B.5 Screening procedure RWS

The screening steps recommended by RWS are:

- Evaluate excitation due to turbulence and vortex shedding
    - Horizontal direction
    - Vertical direction
- Evaluate excitation due to flow instabilities at the bottom edge
- Evaluate excitation due to motion induced instabilities
- Evaluate potential enhancement via resonances

This list is complete but lacks perhaps in the screening of self-excited mechanism. But in principle this list is complete.

B.6 Screening Kaneko

Kaneko mainly covers tubes and tubes, tube bundles and other rectangular cross sections. For cross flow the following steps are recommended for evaluating/screening calculations for a single cylinder and non-circular objects. Double cylinders and tube bundles are covered in the reference handbook but are

deemed less applicable for the current report. Only stable single phase flow is discussed. Again in the reference book oscillating flow and two-phase flow are covered.

The different regimes to be evaluated are:

- Single cylinder – forced vibration due to Karman vortex shedding
- Single cylinder - synchronization with Karman/symmetric vortex shedding
- Single cylinder – turbulence induced vibration
- Single cylinder – vibration induced by tip-vortex in the high flow velocity regime
- Non-circular – vortex-induced vibration
- Non-circular – Turbulence induced vibrations
- Non-circular – galloping

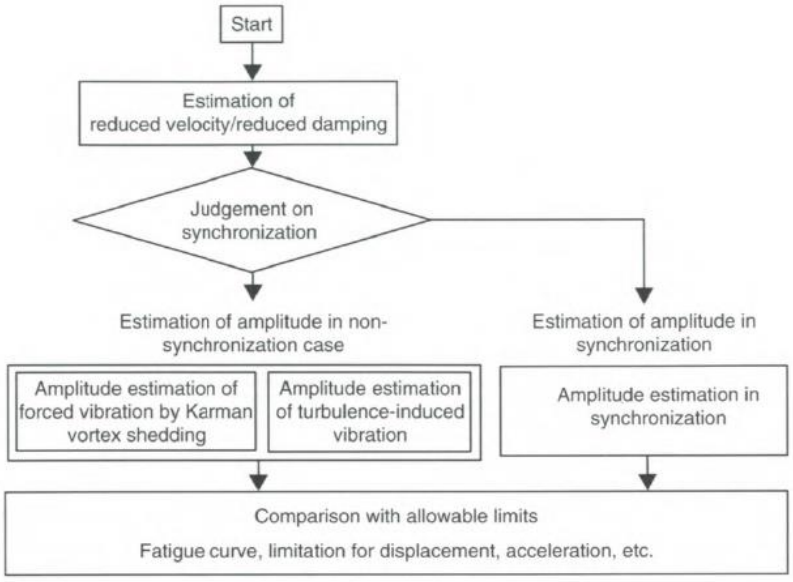

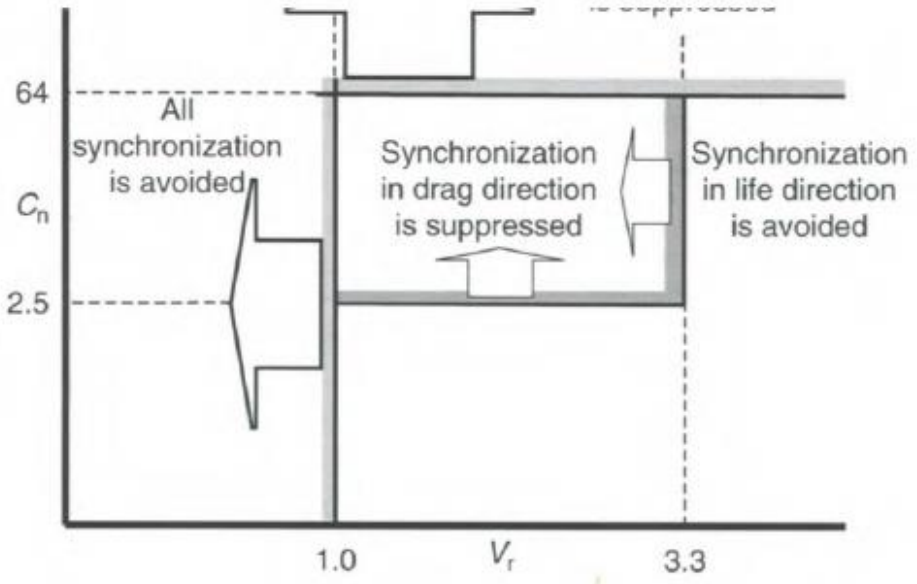

Fig. 2.5 Range of avoidance and suppression of synchronization.

	JSME Guidelines	ASME Guidelines	
	Satisfaction of some requirements is needed		
1	$V_r < 1$	$V_r < 1$	Avoidance
2	$C_n > 64$	$C_n > 64$	Suppression
3	$V_r < 3.3$ and $C_n > 2.5$	$V_r < 3.3$ and $C_n > 1.2$	Avoidance of lift oscill Suppression of drag os
4		$f_0/f_w < 0.7$ or $f_0/f_w > 1.3$	Avoidance of only lift

Figure 48: Classification, screening and evaluation criteria according kenlo (Kan 37 – 39)

C Base graphs turbulent excitation

D Base figures vortex shedding

D.1 Cylinder

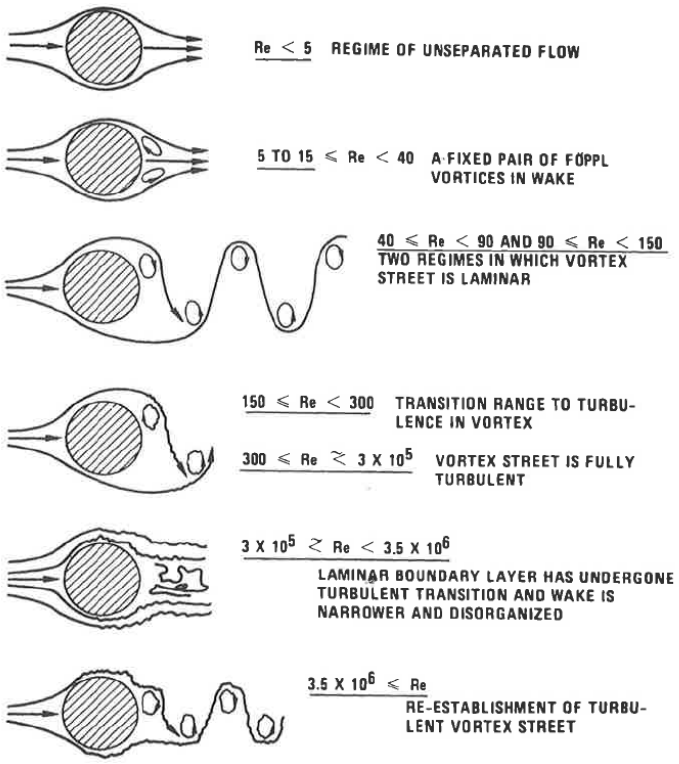

Figure 49: Vortex shedding regimes for a cylinder (Blevins, 2001).

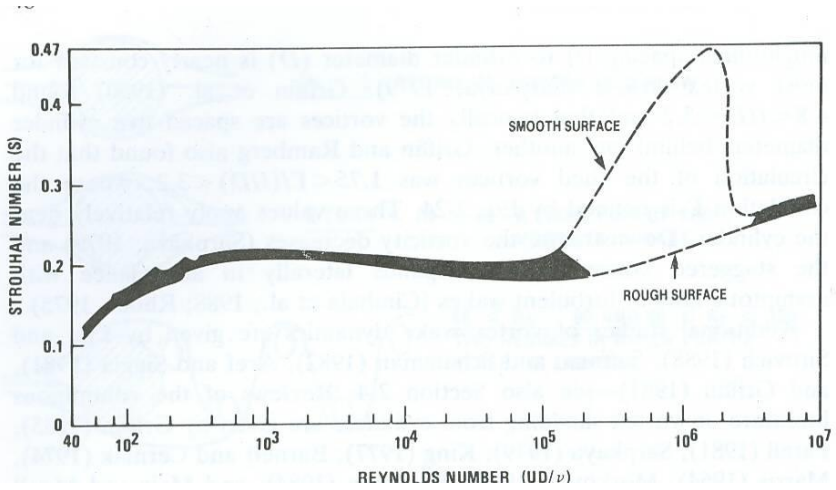

Figure 50: Strouhal number as function of Reynolds number (Blevins, 2001).

D.1.1 Dynamic lift coefficient

$$F_L = \frac{1}{2}\rho U^2 (D \cdot L) C_L \sin(2\pi f_s t)$$

Low Reynolds : C_L ~0.2
Maximum C_L ~1.4

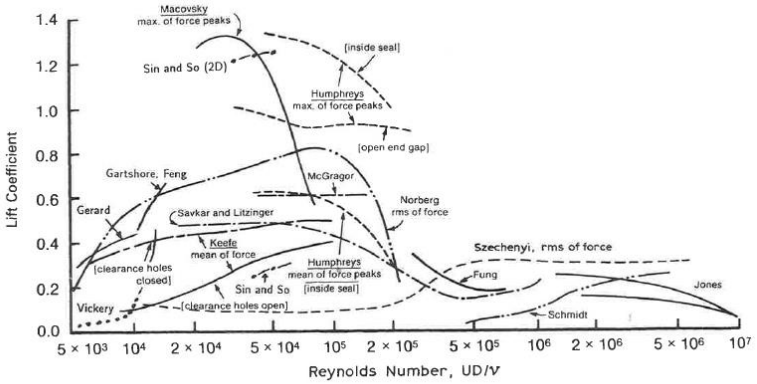

Fig. 3-16 Measurements of vortex-induced lift coefficient on stationary cylinder (Yamaguchi, 1971; Szechenyi, 1975; Jones et al., 1969; Gartshore, 1984; Sin and So, 1987; Savkar and Litzinger, 1982).

Figure 51: Overview of measured lift coefficients as function of Reynolds numbers (Blevins, 2001).

D.1.2 Dynamic drag coefficient

The dynamic drag coefficient of a cylinder is very dependent on the amplitude of the Reynolds number but is typically one order lower than the lift coefficient (~0.05) but is also very dependent on the amplitude of the fluctuations.

D.2 Cavity

The base example is a cavity flow. In an infinite way the cavity will exhibit different modes dependent on the number of vortices in the cavity.

Classically this is given by Rossiter (・ = 0.25 and kv = 0.57):

Sr= (n-ξ)/(1+1/kv)

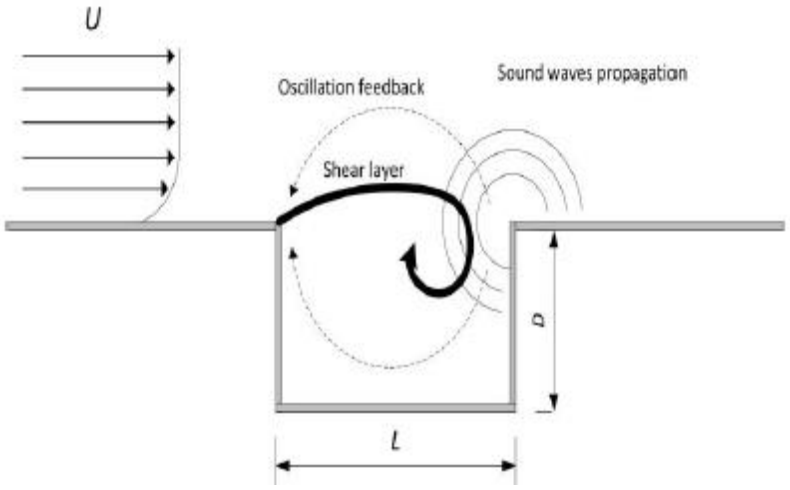

Figure 52: cavity geometry

If this system is subjected to possible acoustic modes there is an interaction between the shear layer modes and the acoustic modes resulting in high amplitude behaviour

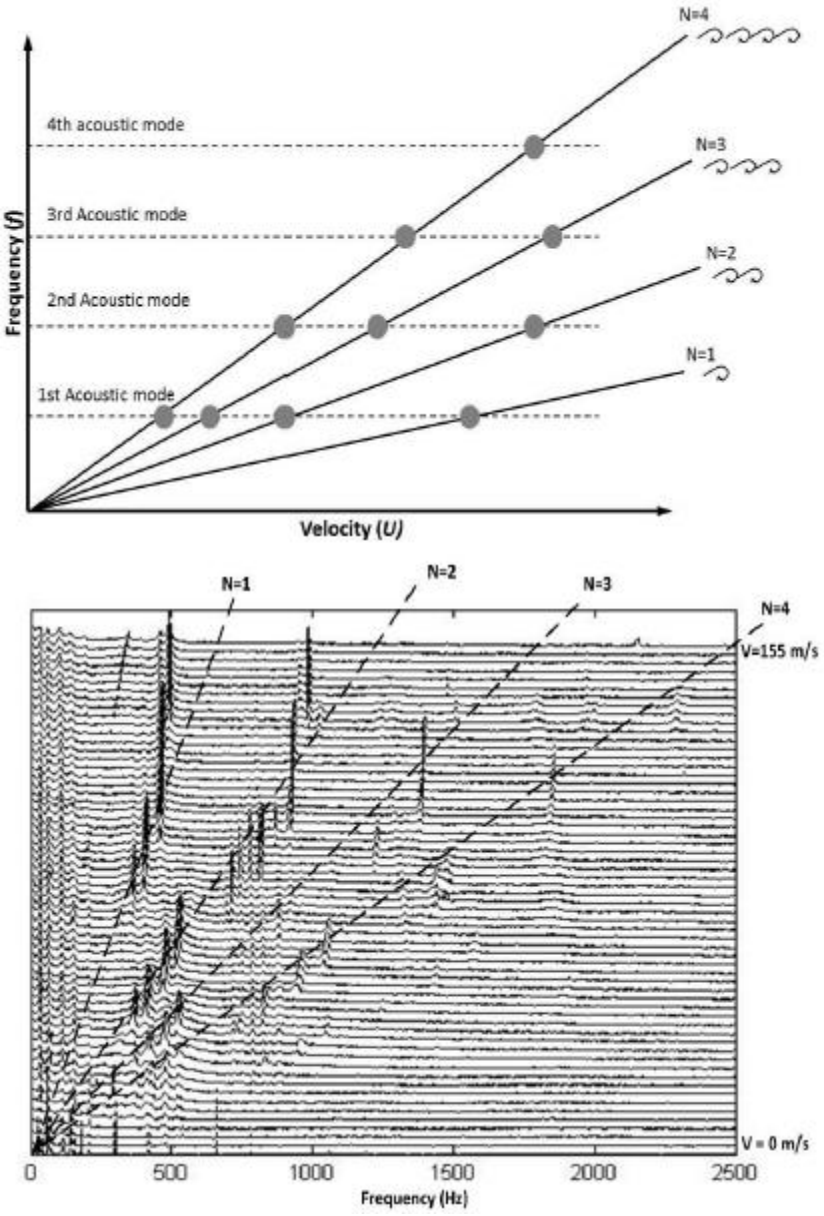

Figure 53: Interaction between cavity and acoustic modes.

D.3 Plates

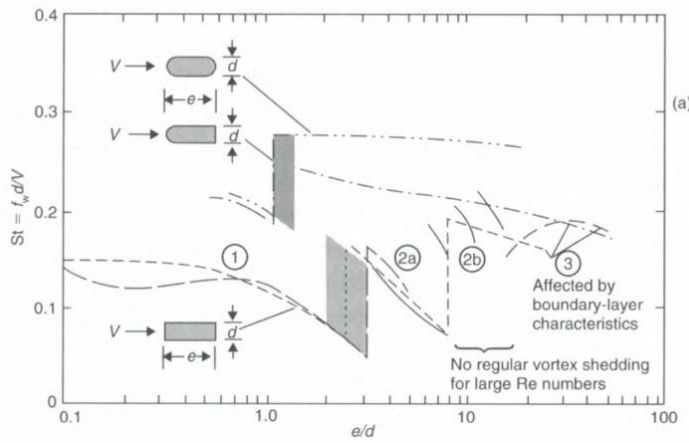

(a) Angle of incidence $\alpha = 0°$: — —, — · — [120] for Tu ≃ 0.2%, $17\,000 < \sqrt{d}/\nu < 35\,000$; - - - [121] for Tu ≃ 0.5%, $720 < \sqrt{d}/\nu < 31\,000$; ———, [122] for Tu ≃ 0.3%, Vd/ν = 1000; — · · — , [123] for Tu ≃ 4.5%, Vd/ν = 1300.

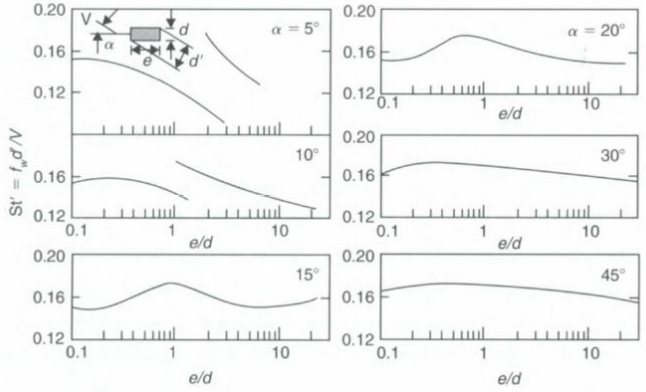

(b) Angle of incidence $5° < \alpha < 45°$ [121].

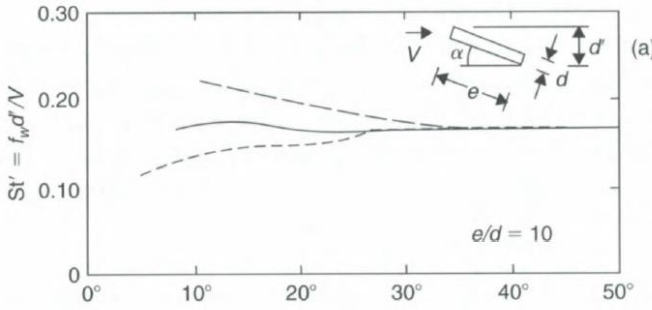

(a) Data for square-edged prism:—, [124] for Tu ≃ 0.8%, $Vd/\nu \simeq 1500$, aspect ratio L/e = 10;- - -, [121] for Tu≃0.5%, $\frac{V_d}{\nu} \simeq 2000$, $L/e = 3.2$;— –, [125] for Tu ≃ 2.4%, $1000 < \frac{V_d}{\nu} < 2500$, $L/e = 8$.

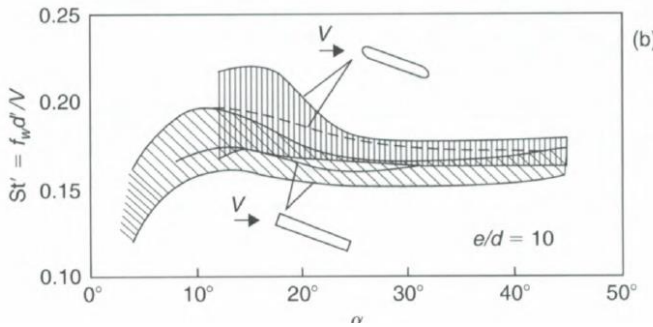

(b) Data for prism with square and rounded edges [124], for $\frac{V_d}{\nu} \simeq 1500$, L/e = 10: ———, - - - -, Tu ≃ 0.8%; ▨, ▨ Tu ≃ 2.1%.

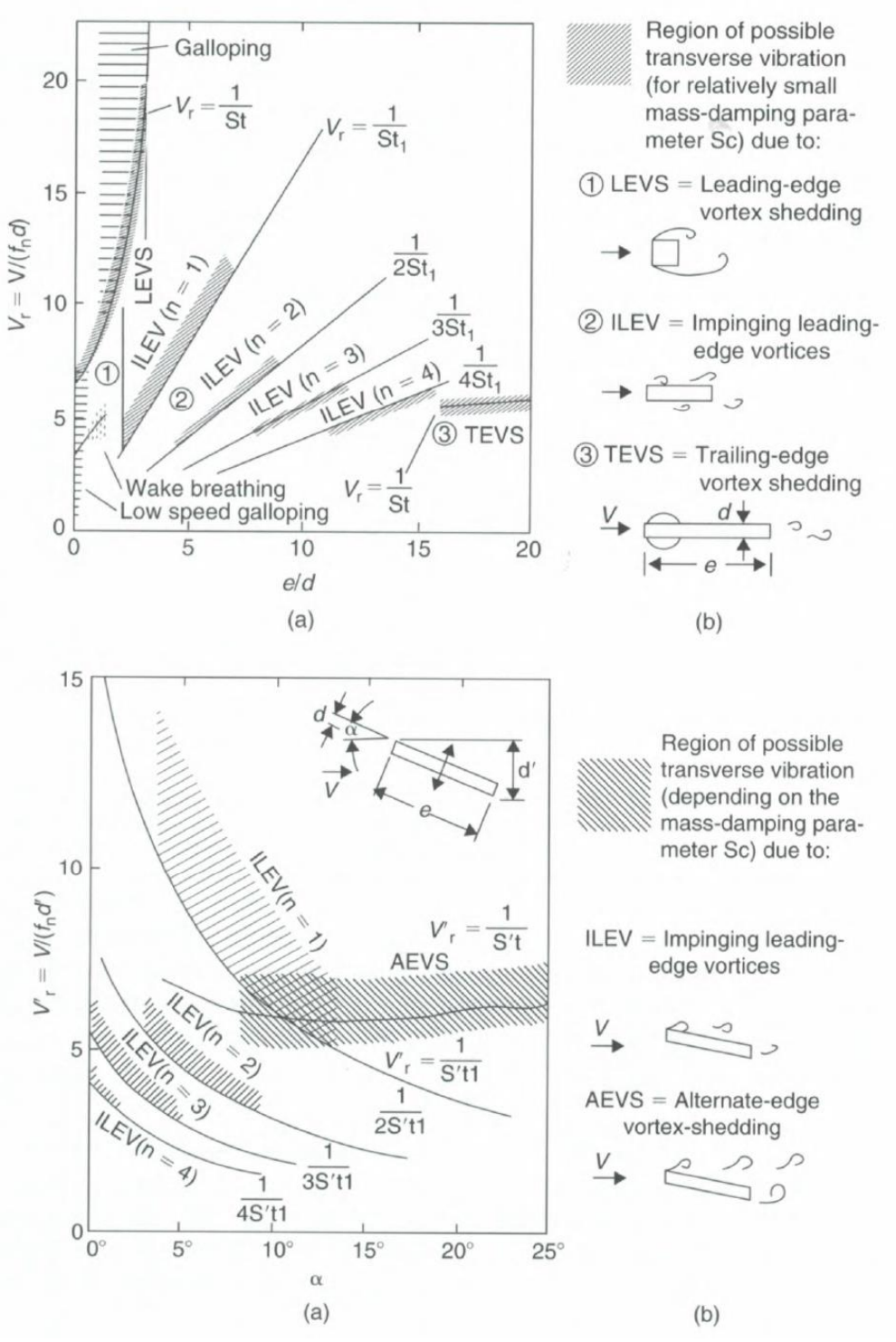

Figure 54: Strouhal number as function of plate aspect ratio, edge rounding and inclination (Kaneko, Nakamura, Inada, & Kato, 2008).

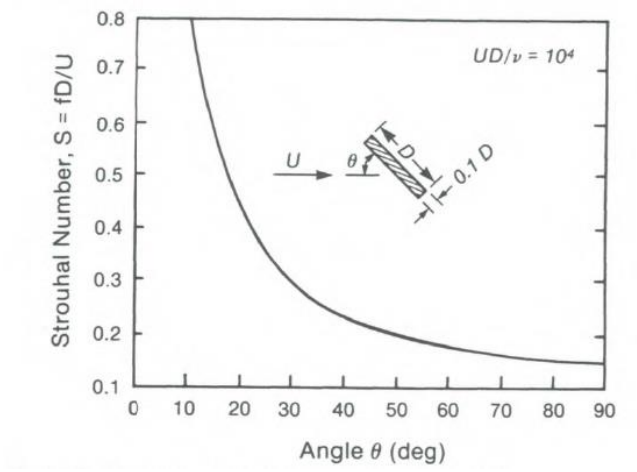

Figure 55: Strouhal number as function of inclination angle (Blevins, 2001). This figures indicates that at larger inclinations the effective length scale will be the length of the plate rather than the thickness of the plate. At zero inclination, the Sr = fD/U should go to approximately Sr = 2.

D.4 General bluff bodies

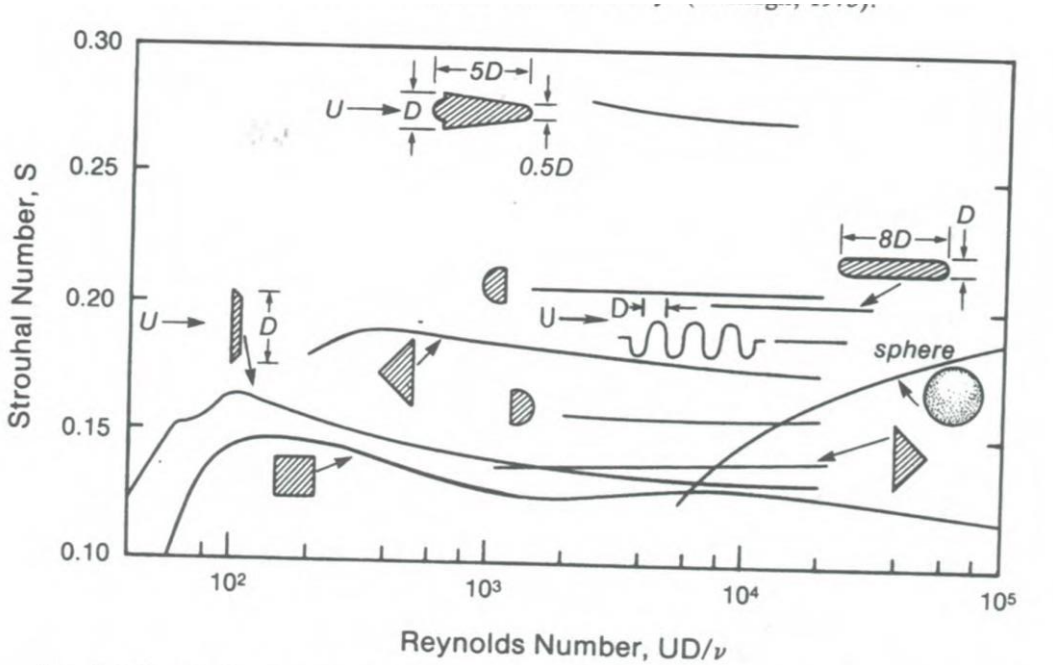

Fig. 3-6 Strouhal numbers for noncircular sections. Flow is left to right (Roshko, 1954; Wardlaw, 1966; Mujumdar and Douglas, 1973; Vickery, 1966; Gerlach, 1972; Toebes and Eagleson, 1961; Okajima, 1982; Achenbach and Heinecke, 1981).

Figure 56: Strouhal number for general bluff bodies (Blevins p50).

E Base figures galloping

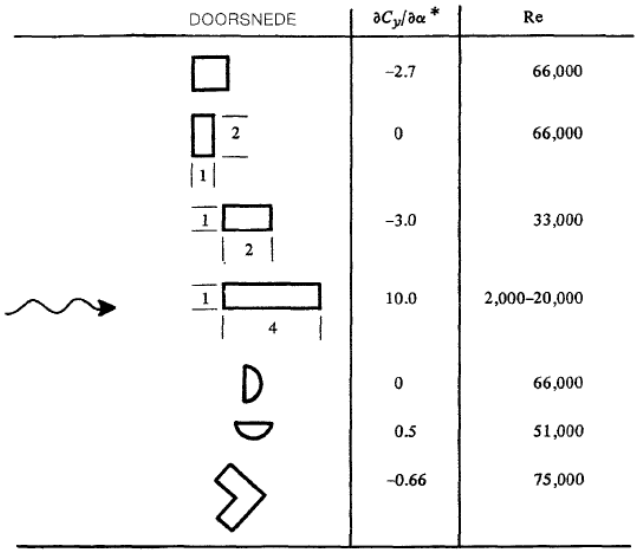

Figuur A5.18:
Doorsneden van staven die gevoelig of juist ongevoelig zijn voor galloping, Blevins (1977).

*) α is in radialen; stroming van links $\partial C_y/\partial\alpha = \partial C_L/\partial\alpha + C_w$.

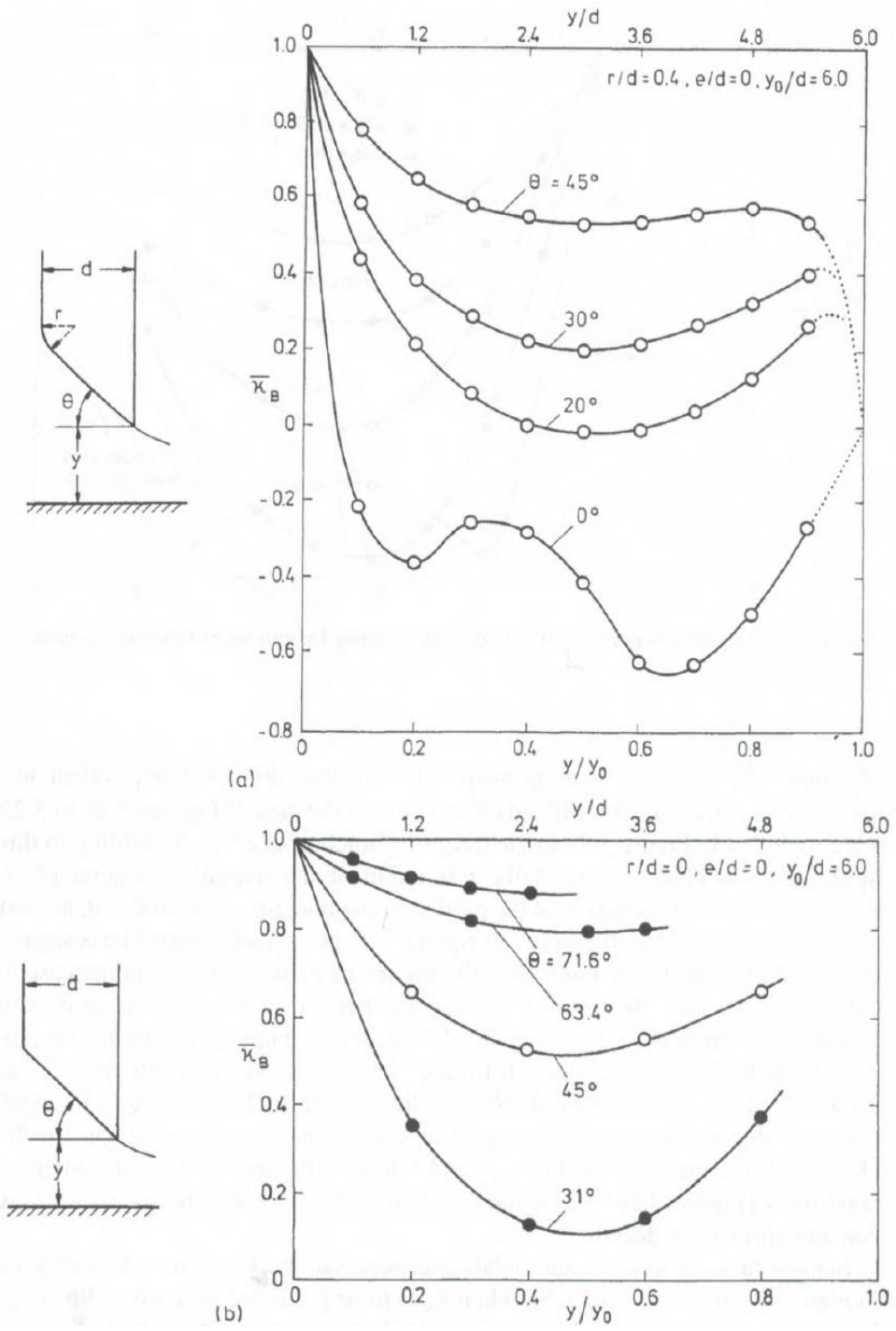

Figure 57: Downpull coefficient κ as function of relative gate height [Nau p 155]. The downpull coefficient is similar to the lift coefficient in behaviour. Critical are regions of dκ/d(y/d) > 0.

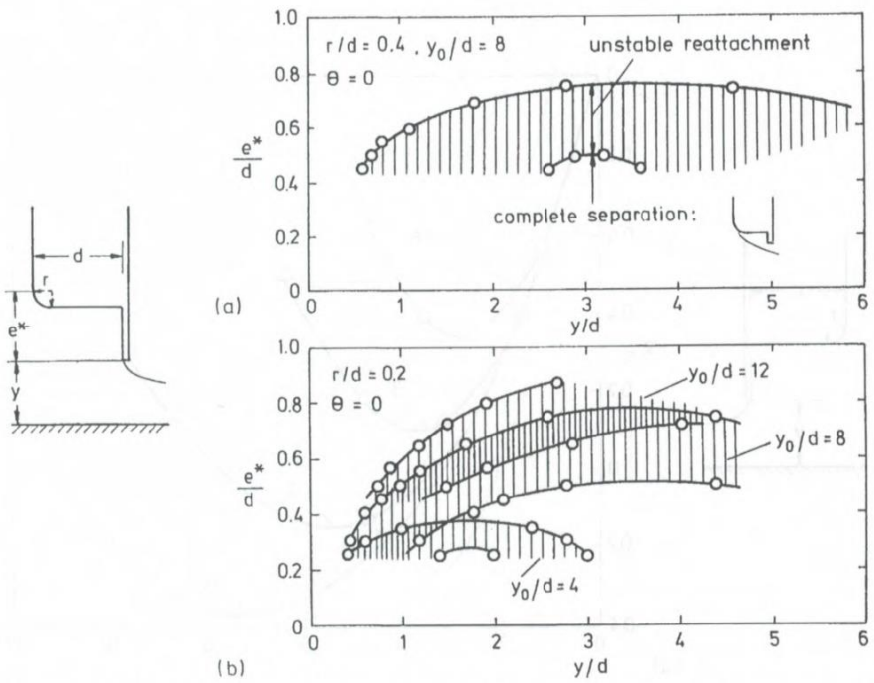

Figure 3.24. Conditions of unstable reattachment of flow on the gate lip as a function of e^*/d and y/d.

lip of a tunnel gate

Figure 58: Stability criterion for lip design [Nau p 160].

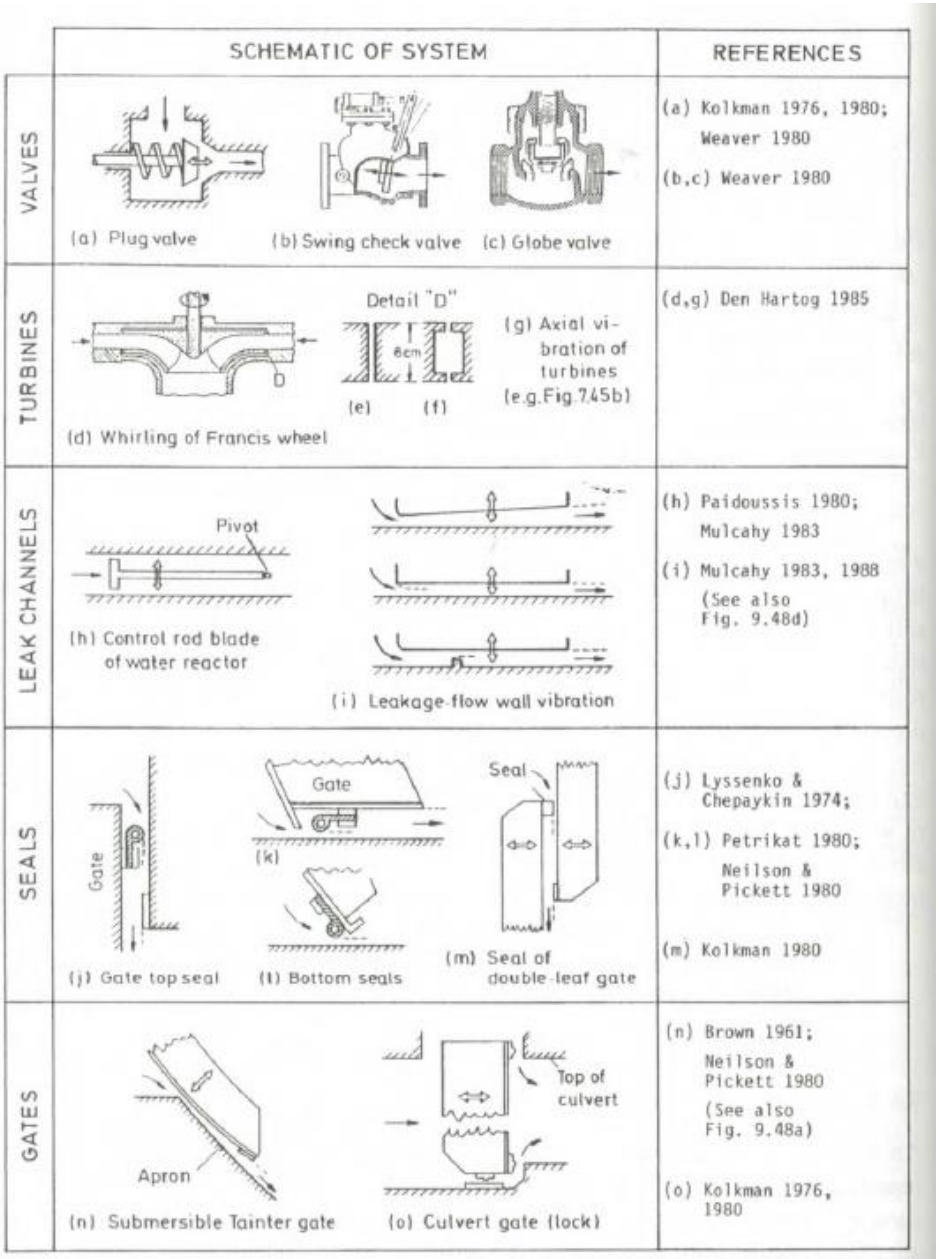

Figure 7.48. Examples of systems susceptible to movement-induced excitation involving coupling with fluid-flow pulsations.

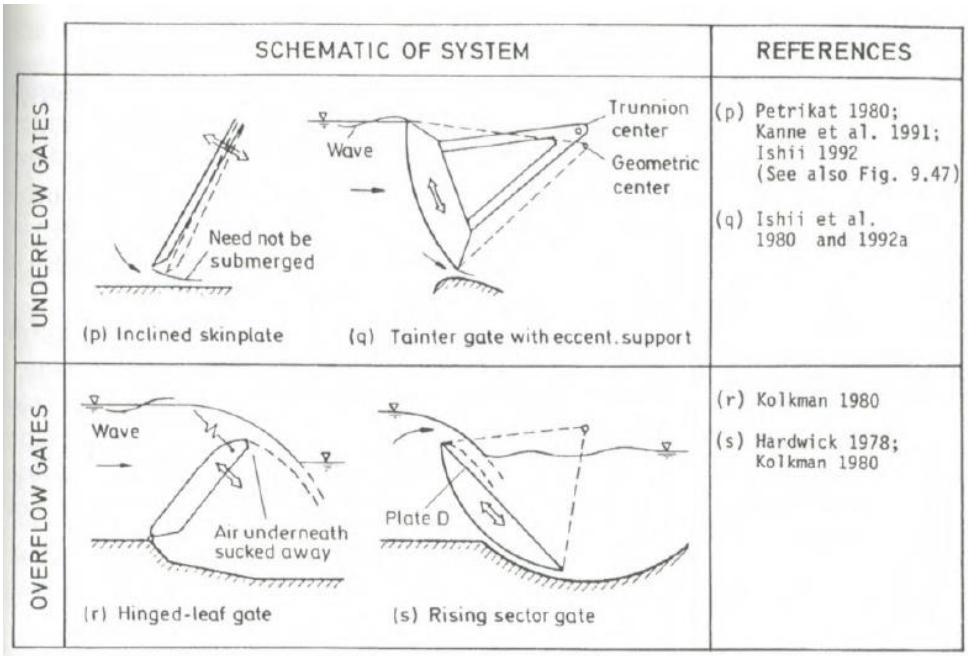

Figure 7.48 (continued). Examples of systems susceptible to movement-induced excitation involving coupling with fluid-flow pulsations.

F Some remarks on added mass.

The added mass concept is a concept in which fluid forces are added to the equation of motion of the body. An added mass must be added to obtain an effective structure mass, because when an item is vibrating in a (still fluid) the fluid around the structure must also be accelerated. The kinetic energy of the moving fluid adds to the kinetic energy of the vibrating item [F.1,F.2].

This additional added mass may be determined from a potential flow model [1]. This requires a dedicated calculation. The added mass can be computed by summing tht total kinetic energy of the fluid relative to the body and setting this equal to an equivalent body energy [F.5]:
$KE_{fluid} = \int \frac{1}{2} dm V_{rel}^2 = \frac{1}{2} m_a U^2$
The integral is the solution of a potential flow calculation. A more complete proof os given in F.6

For a number of simple geometries the added mass coefficients can be found in literature. For example in [F.2]. Please note that due to the added mass there can become a coupling between dimensions. That is a vibration in one direction can result in a force in the perpendicular direction.

Larger discussions on the added mass can be found in Chapter 3.2 [F.3]. A full comprehensive method is given in F.4. A stepwise discussion is given in [F.2] with an example given in K&J C Annex III.

A number of remarks must be made which complicate the analysis:

- The added mass terms depends whether it concerns a stagnant fluid or a moving/accelerating fluid.
- The added mass coefficients are often directional dependent.
- For turbulence and vortex shedding the added mass coefficients are recommended. For use in instability analysis it is recommended to fully couple the fluid and mechanical analysis [F.3 p 45].
- The added mass coefficient will be dependent on the mode shape and on the gate position.

[F.1] H. Goyder, 2017, ‘Natural frequencies and damping of a full-scale pipe loop in air and water’, PVP2017-65402, ASME PVP conference
[F.2] Blevins, 2001,’Flow-Induced Vibrations, 2nd edition’, 2001
[F.3] E. Naudasher, D. Rockwell, 2005, ‘Flow-Induced Vibrations’, Dover Publications.
[F.4] N. Ishii, K. Anami, C.W. Knisely, 2018, ‘Dynamic Stability of hydraulic gates and engineering for flood prevention’, IGI Global
[F.5] F.M. White, 1988,’Fluid Mechanics, second edition’, McGraw-Hil Book Co.
[F.6] M.P. Paidoussis,’2014,’Fluid-Structure Interactions. Slender structures and axial flow. Volume 1, second edition’, Academic press